Permeation of Large Tetra-alkylammonium Cations through Mutant and Wild-Type Voltage-gated Sodium Channels as Revealed by Relief of Block at High Voltage

Chien-Jung Huang,* Isabelle Favre,* and Edward Moczydlowski*‡

From the *Department of Pharmacology and ‡Department of Cellular and Molecular Physiology, Yale University Medical School, New Haven, Connecticut 06520-8066

abstract Many large organic cations are potent blockers of K^+ channels and other cation-selective channels belonging to the P-region superfamily. However, the mechanism by which large hydrophobic cations enter and exit the narrow pores of these proteins is obscure. Previous work has shown that a conserved Lys residue in the DEKA locus of voltage-gated Na^+ channels is an important determinant of Na^+/K^+ discrimination, exclusion of Ca^{2+}, and molecular sieving of organic cations. In this study, we sought to determine whether the Lys(III) residue of the DEKA locus interacts with internal tetra-alkylammonium cations (TAA^+) that block Na^+ channels in a voltage-dependent fashion. We investigated block by a series of TAA^+ cations of the wild-type rat muscle Na^+ channel (DEKA) and two different mutants of the DEKA locus, DEAA and DERA, using whole-cell recording. TEA^+ and larger TAA^+ cations block both wild-type and DEAA channels. However, DEAA exhibits dramatic relief of block by large TAA^+ cations as revealed by a positive inflection in the macroscopic I–V curve at voltages greater than +140 mV. Paradoxically, relief of block at high positive voltage is observed for large (e.g., tetrapentylammonium) but not small (e.g., TEA^+) symmetrical TAA^+ cations. The DEKA wild-type channel and the DERA mutant exhibit a similar relief-of-block phenomenon superimposed on background current rectification. The results indicate: (a) hydrophobic TAA^+ cations with a molecular diameter as large as 15 Å can permeate Na^+ channels from inside to outside when driven by high positive voltage, and (b) the Lys(III) residue of the DEKA locus is an important determinant of inward rectification and internal block in Na^+ channels. From these observations, we suggest that hydrophobic interfaces between subunits, pseudosubunits, or packed helices of P-region channel proteins may function in facilitating blocker access to the pore, and may thus play an important role in the blocking and permeation behavior of large TAA^+ cations and potentially other kinds of local anesthetic molecules.

key words: local anesthetic • ionic selectivity • Na^+ channel • selectivity filter • tetraethylammonium

INTRODUCTION

Tetra-alkylammonium (TAA^+)[1] cations such as TEA^+ are known to inhibit ionic currents through channel proteins by transiently binding in the ion conduction pathway and blocking the flow of current (Tasaki and Hagiwara, 1957; Armstrong and Binstock, 1965; Hille, 1967). The fact that K^+ channels often differ in sensitivity to block by internal and external TAA^+s has led to the picture that these channels have distinct internal and external binding sites for such molecules located in antechambers separated by a narrower tunnel in the middle of the pore that cannot readily be penetrated by large organic cations (Armstrong, 1992;Hille, 1992). Structure–activity studies have identified certain amino acid residues in K^+ channel proteins that influence TEA^+ block (MacKinnon and Yellen, 1990; Kavanaugh et al., 1991; Yellen et al., 1991; Heginbotham and MacKinnon, 1992; Choi et al., 1993). In the crystal structure of a K^+ channel protein (KcsA), residues homologous to those that determine the binding affinity of external and internal TEA^+ in related K^+ channels are located precisely at the respective outer and inner entrances of the narrowest region of the pore called the selectivity filter (Doyle et al., 1998). In the structure of KcsA, this filter is a narrow tunnel that measures ~3 Å in diameter by 12 Å in length.

Voltage-gated Na^+ and Ca^{2+} channels are structurally related to K^+ channels as members of a homologous superfamily of cation-selective channels (Pongs et al., 1988; Jan and Jan, 1990). In particular, these three types of channels share a structural motif called the P-region located between the M1/M2 transmembrane helices of KcsA or between the corresponding S5/S6 presumed helices of voltage-gated K^+, Na^+, and Ca^{2+} channels (MacKinnon, 1995; Moczydlowski, 1998). In all three

Address correspondence to Edward Moczydlowski, Department of Pharmacology, Yale University Medical School, 333 Cedar St., New Haven, CT 06520-8066. Fax: 203-785-7670; E-mail: edward.moczydlowski@yale.edu

[1]*Abbreviations used in this paper:* μ-CTX, μ-conotoxin GIIIB; MA^+, methylammonium; STX, saxitoxin; TAA^+, tetra-alkylammonium; TBA^+, tetrabutylammonium; $THexA^+$, tetrahexylammonium; TMA^+, tetramethylammonium; TPA^+, tetrapropylammonium; $TPeA^+$, tetrapentylammonium; TTX, tetrodotoxin.

types of channels, specific conserved residues in the P-region determine ionic selectivity (Heinemann et al., 1992; Yang et al., 1993; Heginbotham et al., 1994). The structure of KcsA revealed that K^+ selectivity in tetrameric K^+ channels originates from a K^+-binding region consisting of four rings of carbonyl oxygen atoms of the peptide backbone contributed by residues of a strongly conserved signature sequence. However, many studies indicate that the mechanism of ionic selectivity and the structure of the analogous selectivity filter are likely to be quite different for Na^+ and Ca^{2+} channels versus K^+ channels. Ionic selectivity in pseudotetrameric Na^+ and Ca^{2+} channels is known to be intimately related to a set of mostly charged residues located near the outer mouth of the pore (Heinemann et al., 1992; Yang et al., 1993; Favre et al., 1996). These residues are called the EEEE locus in Ca^{2+} channels and the DEKA locus in Na^+ channels. The notation EEEE/DEKA corresponds to the single letter code for conserved amino acid residues that can be readily aligned in homologous domains I, II, III, and IV of Ca^{2+}/Na^+ channels, respectively. In a preceding study from our laboratory, the conserved Lys residue in domain III of the DEKA locus of Na channels, K(III), was identified as a major determinant of the molecular sieving behavior of the rat skeletal muscle Na-channel (μ1) with respect to organic cations (Sun et al., 1997). Mutation of this Lys residue to Ala, as in the mutation of DEKA to DEAA, produces a channel that is permeable to many organic cations ranging in size from methylammonium (3.8-Å diameter) to TEA^+ (8.2-Å diameter), as demonstrated by direct measurement of inward currents carried by these cations. This latter behavior is quite different from native Na^+ channels, which are effectively impermeable to external organic cations larger than guanidinium, a fact that has been used to establish 3.2 $\times$ 5.2 Å as the cutoff area of the narrowest cross-section of the native pore (Hille, 1971, 1972).

The enhanced permeability of the DEAA mutant to large organic cations provides a unique opportunity to explore the mechanism of block by TAA^+ cations and related local anesthetic drugs that are known to preferentially block voltage-gated Na^+ channels from the intracellular side. If the K(III) residue of the DEKA locus corresponds to the location of a major energy barrier for the movement of large cations through the pore, then lowering this energy barrier by mutation may enhance the permeability of blocking cations that enter the channel from the inside. Alternatively, if other significant energy barriers are located between the DEKA locus and the intracellular pore entrance, then such mutant Na^+ channels may exhibit asymmetric permeability to organic cations. On this basis, we hypothesized that removal of a structural element such as a Lys residue that limits conduction of organic cations may reveal or enhance a phenomenon known as voltage-dependent relief of block (French and Wells, 1977; French and Shoukimas, 1985), in which a large positive voltage applied on the same side as a cationic blocker allows such blocking ions to permeate through the channel. To address the question of whether the K(III) residue of the DEKA locus corresponds to such an energy barrier, we studied internal block of a DEAA mutant Na^+ channel by a series of symmetrical TAA^+s ranging in size from tetramethylammonium (TMA^+) to tetrahexylammonium ($THexA^+$). We found that internal block of outward alkali cation current through the DEAA mutant by large TAA^+ cations such as tetrapentylammonium ($TPeA^+$) is indeed relieved in a steeply voltage-dependent fashion. Paradoxically, this effect is enhanced for large versus small TAA^+ derivatives, implying that hydrophobic interactions with long *n*-alkyl groups actually facilitate the voltage-driven permeation of very large organic cations through this aqueous pore. In addition, we find that the wild-type Na^+ channel and a DERA mutant, in which the K(III) residue is replaced by Arg, also exhibit voltage-dependent relief of block by large chain TAA^+s, but with apparently different efficiency. The results show that a positively charged residue at the K(III) position of the DEKA locus is not an absolute structural impediment to the movement of large cations through the pore. Implications of these findings for the interpretation of molecular sieving studies of Na^+ channels and blocking interactions of TAA^+ cations are discussed.

MATERIALS AND METHODS

Expression of Wild-Type and Mutant Na^+ Channels

Na^+ channels studied in this paper are the wild-type μ1 rat skeletal muscle isoform (Trimmer et al., 1989) and two mutants of this clone that contain substitutions, K1237A or K1237R. The wild-type and the latter two mutants are referred to, respectively, as DEKA, DEAA, and DERA according to the single letter code for residues in domains I–IV of the DEKA locus, a conserved region in Na^+ channels that aligns with the EEEE locus of Ca^{2+} channels (Heinemann et al., 1992; Sun et al., 1997). DEKA and DEAA clones were studied in stably transfected human fibroblast HEK293 cells. The DERA clone was studied in HEK293 cells that were transiently transfected with a DERA/pcDNA3 vector using Effectene reagent (QIAGEN Inc.). Construction of the mutations, subcloning into pcDNA3 expression vector, and other methods for transfection, generation, and propagation of stable cell lines have been described in previous publications (Favre et al., 1996; Sun et al., 1997).

Solutions and Electrophysiology

The standard extracellular Na^+ bath solution was (mM) 140 NaCl, 3 KCl, 2 $MgCl_2$, 2 $CaCl_2$, 10 glucose, and 10 HEPES-NaOH, pH 7.3. The standard intracellular Cs^+/Na^+ pipette solution was (mM) 125 CsF, 2 $MgCl_2$, 1.1 EGTA, 10 glucose, 20 Na^+-HEPES, pH 7.3. Intracellular pipette solutions containing tetrapropylammonium (TPA^+), tetrabutylammonium (TBA^+), $TPeA^+$, $THexA^+$, and QX-314$^+$ were prepared by adding these blockers to standard Cs^+/Na^+ pipette solution at the desired concentration. The composition of other solutions for testing permeability

to external TEA^+, TMA^+, MA^+, and Ca^{2+} or block by internal TEA^+ are given in the figure legends.

Patch-clamp electrodes were constructed with a commercial pipette puller using Kimax 50 borosilicate capillary glass (Fisher Scientific Co.) without additional fire polishing. The measured pipette resistance was 1–2 MΩ when filled with standard Cs^+/Na^+ pipette solution. Whole-cell voltage-clamp recording was performed at room temperature (~22°C) using an amplifier (EPC-9; HEKA Electronik) with Pulse and Pulse-fit software (Instrutech Corp.). Stably transfected HEK293 cells were seeded for growth on glass cover slips and used for electrophysiological recording within 12–36 h. Transiently transfected cells expressing the DERA mutant channel were used for recording 48 h after transfection. The peak inward current in standard Na^+ bath solution and Cs^+/Na^+ pipette solution of typical cells selected for recording DEKA, DEAA, and DERA current was −4.3 ± 0.4 nA (mean ± SEM, n = 6), −4.1 ± 0.7 nA (n = 12), and −1.6 ± 0.4 nA (n = 5), respectively. Cancellation of residual capacitance transients and linear leak subtraction was carried out using a programmed P/4 negative pulse protocol delivered at −120 mV. The series resistance compensation function of the amplifier was routinely used at 74–79% compensation to minimize voltage error. Nevertheless, some experiments for the DEAA mutant (e.g., see Figs. 2 and 5) involved measurements of outward currents as large as 50–100 nA at the highest positive voltage (+200 mV). In such cases, the effect of voltage errors on our analysis and interpretation was minimized by discarding data sets from cells that exhibited >50 nA of outward current at +200 mV. In addition, the effect of voltage error due to series resistance, R_S, was estimated for the data of Figs. 2 and 5 by correcting the applied voltage by the voltage drop across the noncompensated fraction, f_N, of measured R_S (2.3 ± 0.2 MΩ, n = 5), using Ohm's Law, $\Delta V = If_N R_S$ (Marty and Neher, 1995).

Current–voltage data were collected by recording responses to a consecutive series of step voltage pulses increasing by +10 mV from a holding potential of −120 to +200 mV with a pulse duration of 10 ms. The interval between consecutive voltage pulses was 0.5 or 1 s as noted, except in experiments where it was varied from 0.5 to 10 s for investigation of use-dependent block. Data collection was begun 10 min after whole cell break-in when inward Na^+ current reached a relatively stable level after intracellular perfusion. Data were collected during continuous gravity-fed perfusion of the extracellular bath solution using a commercial patch perfusion chamber (Warner Instrument Co.).

The permeability of extracellular TEA^+ and MA^+ was investigated by measuring the change in reversal potential, ΔV_R, upon changing the extracellular solution from the standard Na^+ bath solution to a different solution containing the cation of interest (e.g., see Figs. 1 A and 7). Permeability ratios of these extracellular cations relative to Na^+ were calculated by the method of Hille (1971) using ΔV_R values corrected for junction potentials and equations described previously (Sun et al., 1997).

Data Analysis and Modeling

Peak current values were measured and plotted as a function of the pulse voltage. In compiling the results, peak I-V data was often normalized by dividing the measured current by the maximum inward current of a given cell. Such data sets collected from three to eight cells were then averaged and plotted as the mean normalized current with error bars given (±SEM).

In Fig. 2 B (below), current values for 10 and 50 μM internal $TPeA^+$ were normalized by dividing each point by the expected peak inward current in the absence of internal $TPeA^+$. The magnitude of the unblocked current was estimated by fitting data points at voltages less than +80 mV to a simple model of voltage-dependent block as described by Eqs. 1 and 2 with outward permeation of the blocker disregarded by setting k_{-2} equal to 0. This procedure yields a reasonable estimate of the maximal conductance, G_{max}, in the absence of blocker. This estimate of G_{max} is then used to generate an I-V relation for the expected unblocked current by setting the blocker concentration, $[B_{in}]$, equal to zero in Eq. 1. The absolute value of the maximal expected inward current is then used to normalize the measured current in the presence of internal $TPeA^+$ to produce a macroscopic I-V curve that is appropriately scaled with respect to that expected in the absence of an internal blocker. This procedure is mathematically similar to that used in Figure 5 of O'Leary and Horn (1994), which describes the blocking effect of internal TEA^+, TPA^+, and TBA^+ on the human heart Na^+ channel as measured by whole-cell recording.

Nonlinear regression fitting of peak I-V data to the model of Scheme I using Eqs. 1 and 2 was performed using the Marquardt-Levenberg algorithm as part of the Sigmaplot 4.0 software package (SPSS Inc.).

Materials

Chloride salts of TAA^+ cations were purchased from Aldrich Chemical Co. (TPA^+, TBA^+, $TPeA^+$) or Sigma Chemical Co. (TEA^+, $THexA^+$). Saxitoxin and tetrodotoxin were purchased from Calbiochem Corp. μ-Conotoxin GIIIB was obtained from Bachem. The quaternary lidocaine derivative QX-314^+ was obtained from Alomone Laboratories.

RESULTS

Voltage-gated Na^+ channels are preferentially blocked by many different hydrophobic organic cations from the intracellular side. For example, QX-314^+, the quaternary ammonium derivative of lidocaine, a local anesthetic, readily blocks Na^+ channels when present on the intracellular side of axons, cells, or planar bilayers (Strichartz, 1973; Moczydlowski et al., 1986; Wang, 1988; Gingrich et al., 1993; Zamponi et al., 1993). Various measurements of the steady state voltage dependence of block of open Na^+ channels by QX-314^+, TAA^+ derivatives, and related molecules, indicate that there is an internal site (or sites) for organic cations that senses 40–70% of the applied voltage from the inside of the membrane (Yamamoto and Yeh, 1984; Wang et al., 1991; Gingrich et al., 1993; French et al., 1998). At the opposite side of Na^+ channels, there is another blocking site for guanidinium toxins such as tetrodotoxin (TTX) and saxitoxin (STX). Amino acid residues that determine the affinity for TTX/STX binding are located at or close to the COOH-terminal side of residues that comprise the DEKA locus, an apparent ring-like structure of mostly charged residues that control the relative permeability to Na^+, K^+, and Ca^{2+} (Terlau et al., 1991; Heinemann et al., 1992). The D, E, and K, residues of the DEKA locus also determine molecular sieving properties of the μ1 Na^+ channel as monitored by inward current carried by various organic cations in the extracellular solution (Sun et al., 1997). This suggests that the DEKA locus forms a constricted region that separates the toxin binding site on the outside

from the blocking site for TAA^+ cations on the inside. If the DEKA locus forms such a constriction in structural terms, or is the major energy barrier in kinetic terms, then one might expect that internal organic cations would become permeable or lose their blocking efficiency in a mutant such as DEAA that displays enhanced permeation of organic cations from the outside. To test this idea, we first examined whether internal organic cations can carry outward currents in the DEAA mutant expressed in HEK293 cells.

Asymmetry of Organic Cation Permeation through the DEAA Mutant Na^+ Channel

The control experiment of Fig. 1 shows that replacement of a standard extracellular Na^+ solution with a solution containing TEA^+ as the major external cation results in a small inward current and a negative shift of the reversal potential of whole-cell peak current for the DEAA mutant. The magnitude of this shift (-24.6 ± 0.3 mV) corresponds to a permeability ratio of $P_{TEA}(out)/P_{Na} = 0.37 \pm 0.01$ ($n = 4$), confirming that external TEA^+ can permeate through this channel. TEA^+ is the largest cation that has thus far been found to exhibit measurable inward current for the DEAA mutant (Sun et al., 1997). When the standard intracellular solution containing 125 mM Cs^+ plus 20 mM Na^+ was replaced with a pipette solution containing 115 mM TEA-Cl, outward current could not be satisfactorily resolved since it was <0.1 nA at $+200$ mV. This observation suggests that the DEAA channel is essentially impermeable to internal TEA^+. To improve the possibility of observing outward current carried by an organic cation, we tested TMA^+, a smaller TAA^+ derivative. Fig. 1 B shows typical currents and peak I-V data obtained for cells recorded in the presence of 115 mM internal TMA^+ and 145 mM external Na^+. This experiment successfully resolved a small outward current carried by TMA^+, but strong rectification observed in the positive voltage range implies that the conductance supported by internal TMA^+ is small in comparison with external Na^+. The nominal reversal potential in this experiment corresponds to a permeability ratio of $P_{TMA}(in)/P_{Na}$ of 0.07, or at least sevenfold less[2] than the value of $P_{TMA}(out)/P_{Na} = 0.50$ that was previously measured with TMA^+ on the outside of the DEAA mutant (Sun et al., 1997). These results indicate that permeation of small TAA^+ cations through the DEAA mutant is asymmetric in nature. TMA^+ carries current through this channel in both directions, but both TMA^+ and TEA^+ are significantly more permeable when tested in the inward versus the outward direction.

Relief of Block by Internal $TPeA^+$ at High Positive Voltage in DEAA Mutant and Wild-Type Na^+ Channels

The next question we addressed was whether block of outward alkali cation current by large hydrophobic TAA^+s is altered in the DEAA mutant compared with wild type. Internal $TPeA^+$ has been previously characterized as a potent blocker of outward Na^+ current for the wild-type human heart Na^+ channel (O'Leary et al., 1994; O'Leary and Horn, 1994). In this latter study, block was described by voltage-dependent binding of $TPeA^+$ to a site located at an apparent electrical distance of 0.41 from the inside with a K_d of 9.8 μM at 0 mV. Fig. 2 shows typical currents and peak I-V data for HEK293 cells expressing the DEAA mutant. Current records obtained under control conditions with 120 mM Cs^+ plus 20 mM Na^+ in the internal solution were compared with similar recordings with 1, 10, or 50 μM $TPeA^+$ added to the pipette solution. The control records show that large rapidly inactivating outward currents are observed under these conditions. The outward current is a mixture of Cs^+ and Na^+ current since this mutant is rather nonselective for alkali cations with $P_{Cs}/P_{Na} = 0.57$ for Cs^+ tested on the outside (Sun et al., 1997). The control peak current in the DEAA mutant exhibits nearly ohmic behavior in the positive voltage range up to $+200$ mV (Fig. 2 B, control). Fig. 2 B shows that addition of 10 or 50 μM $TPeA^+$ to the internal solution strongly suppresses outward current carried by alkali cations. In the positive voltage range up to about $+140$ mV, $TPeA^+$ behaves as a voltage-dependent blocker as reported for the heart Na^+ channel (O'Leary et al., 1994).

However, at voltages greater than $+140$ mV, there is a sharp upturn of the peak I-V relationship with 10 and 50 μM $TPeA^+$ (Fig. 2 B). Inspection of the corresponding current traces (Fig. 2 A) shows that outward currents recorded with 10 and 50 μM $TPeA^+$ display typical rapid activation and inactivation kinetics of voltage-gated Na^+ channels. A positive inflection in the peak I-V relations of Fig. 2 B arises from a rather abrupt increase in transient current at voltages greater than $+140$ mV (Fig. 2 A). This kind of behavior is consistent with voltage-dependent relief of $TPeA^+$-blocked Na^+ channels, rather than an artifact due to activation of

[2]This estimate of 0.07 for $P_{TMA}(in)/P_{Na}$ was calculated using the apparent reversal potential and an appropriate form of the Goldmann-Hodgkin-Katz voltage reversal equation for major monovalent cations. However, this calculation does not take into account the change in junction potential that occurs in whole-cell recording after diffusional equilibration between the pipette contents and cell interior. As described by Marty and Neher (1995), the actual membrane potential will be more positive than the amplifier reading when the dominant cation (TMA^+) in the pipette solution is less mobile than the dominant anion (Cl^-). This means that the true reversal potential in this experiment is more positive than the measured value and that our estimate of the relative permeability of TMA^+(in) is an upper limit. Thus, this uncertainty does not compromise the conclusion that internal TMA^+ has lower permeability than external TMA^+.

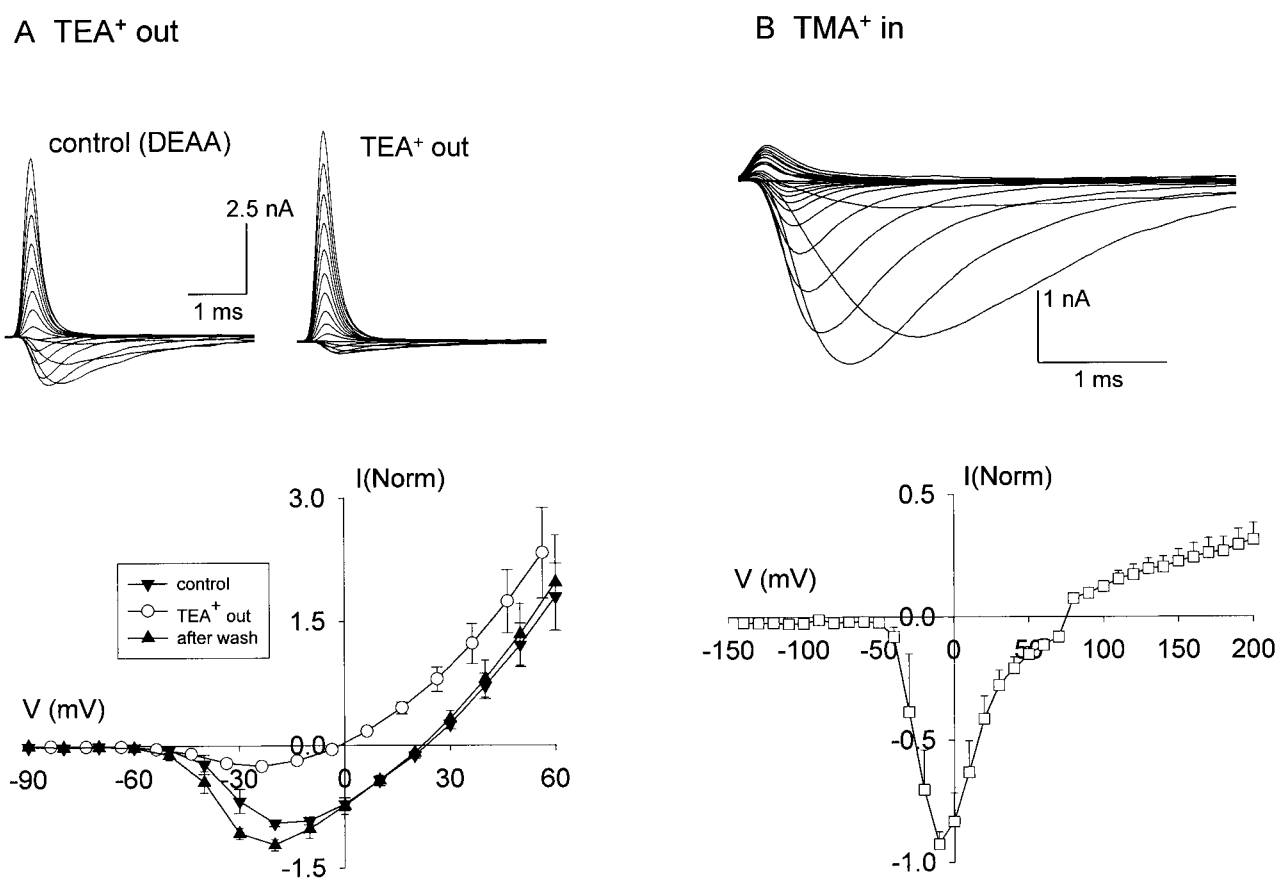

Figure 1. Permeation of external TEA^+ and internal TMA^+ as observed for the DEAA mutant. Whole-cell currents were recorded with a series of consecutive 10-ms voltage steps of +10 mV from a holding potential of −120 mV at intervals of 1 s. (A) External TEA^+ carries a small inward current. (Top) Typical records with standard Cs^+/Na^+ pipette solution and standard Na^+ bath solution before (left) and after (right) perfusion with TEA^+ bath solution (143 mM TEA-Cl, 2 mM $MgCl_2$, 2 mM $CaCl_2$, 10 mM glucose, 10 mM HEPES-TEA, pH 7.3). (Bottom) Normalized peak I-V curves (mean of four cells ± SEM) in control Na^+ bath solution, after replacement with TEA^+ bath solution, and again after washout of TEA^+ with Na^+ solution. (B) Internal TMA^+ carries a small outward current. (Top) Typical currents with TMA^+ pipette solution (100 mM TMA-Cl, 2 mM $MgCl_2$, 1.5 mM EGTA, 10 mM glucose, 20 mM HEPES-TMA, pH 7.3) and standard Na^+ bath solution. Peak-normalized I-V data are shown at the bottom (mean of three cells ± SEM). Solid lines simply connect I-V data points in Figs. 1–8 and do not signify any particular theory.

some other type of channel with different kinetics in HEK293 cells. Visual comparison of the time course of the outward current in the absence and presence of $TPeA^+$ shows that the apparent rate of inactivation is distinctly faster with $TPeA^+$ (Fig. 2 A). This phenomenon was also observed by O'Leary et al. (1994) and O'Leary and Horn (1994), who concluded that the fast component of inactivation in the presence of internal $TPeA^+$ is related to the rate of association of $TPeA^+$ to the open channel. Such changes in the kinetics of Na^+ currents by TAA^+ cations are interesting but beyond the scope of the present study. Here we focus on the mechanism of relief of block as assayed by the magnitude of peak current.

Because the absolute outward current in HEK293 cells expressing the DEAA mutant can be as large as 100 nA, we considered whether residual series resistance error might lead to distortions in the measured peak I-V relations that could affect our interpretation. Uncompensated series resistance leads to distortions in the current time course and a failure to maintain the desired clamp voltage (Armstrong and Gilly, 1992; Marty and Neher, 1995). This voltage error is proportionally greater, the greater the current. In Figs. 2 B and 5 B, we show the probable effect of this error on the measured peak I-V relations by correcting the applied voltage by the estimated voltage drop due to uncompensated series resistance. The greatest effect of this error is an underestimation of the actual magnitude of the peak current at high positive voltages. Since absolute current recorded in the presence of blockers is substantially reduced relative to control, this error actually results in a greater distortion of the control records without blockers than the records taken in the presence of $TPeA^+$. Also, this error leads to an underestimate of the true slope of the peak I-V relation in the high voltage

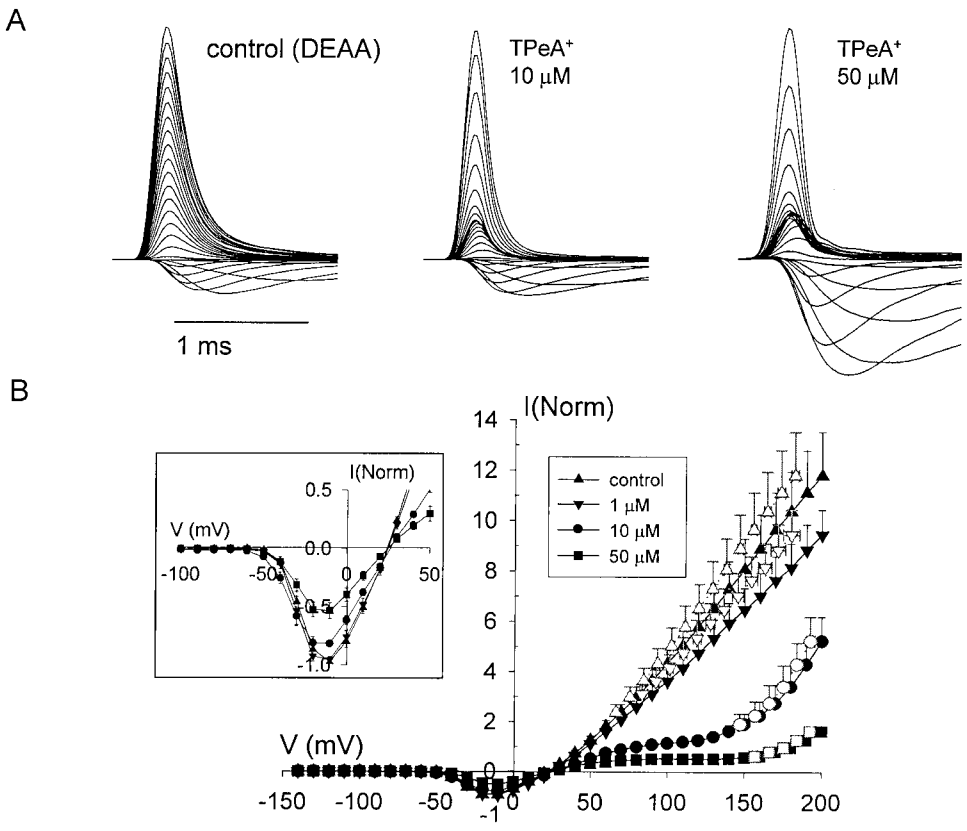

Figure 2. Block and relief-of-block at high positive voltage by internal $TPeA^+$ as observed for the DEAA mutant. The voltage pulse protocol is the same as that of Fig. 1 at pulse intervals of 0.5 s. (A) Typical current records with standard Cs^+/Na^+ pipette solution and standard Na^+ bath solution in the absence (left) and presence of 10 μM (middle) and 50 μM (right) $TPeA^+$ in the pipette solution. Currents traces for different conditions are normalized to maximum peak outward current in the absence of $TPeA^+$. (B) Relative I-V behavior of the DEAA mutant with 0, 1, 10, and 50 μM internal $TPeA^+$. I-V data for 0 and 1 μM $TPeA^+$ are normalized relative to the peak inward current of a given cell before averaging. Similarly normalized I-V data for 10 and 50 μM $TPeA^+$ are scaled relative to the expected maximal conductance of a control cell without $TPeA^+$ based on the fitted level of voltage-dependent block in the voltage range less than +80 mV (see materials and methods). The inset is an expanded view of data in the negative voltage range. Closed symbols are plotted versus nominal applied voltage. Open symbols represent approximate corrections of applied voltage for series resistance error at large voltage steps. Data points are the mean ± SEM for three to five cells.

range. Thus, data distortion caused by series resistance error cannot explain the dramatic upturn in the peak I-V relations measured in the presence of $TPeA^+$.

An inconvenient aspect of quantitative analysis of internal blockers by whole-cell patch clamp is that the internal solution cannot be readily changed, so that the level of unblocked control current for a given cell with internal blocker is difficult to establish. However, since TAA^+ cations are well behaved voltage-dependent blockers of Na^+ channels in the low voltage range of +80 mV or less (O'Leary and Horn, 1994) and the control outward current of the DEAA mutant is fairly ohmic, it is possible to estimate the fractional amount of current inhibition from the known blocking behavior. For example, in Fig. 2 B, data for 10 and 50 μM $TPeA^+$ were normalized to the unblocked current expected for each cell in the absence of $TPeA^+$ by a procedure that involved fitting data in the low voltage range to a simple Boltzmann model of voltage-dependent block (see materials and methods). Thus, the I-V data for 0, 10, and 50 mM $TPeA^+$ are displayed in a way that reflects the underlying concentration dependence of current inhibition in the presence of $TPeA^+$. When viewed in this fashion, the results of Fig. 2 strongly suggest that the positive inflection in the I-V data for 10 and 50 mM internal $TPeA^+$ arises from genuine relief of block due to voltage-driven permeation of this blocker through the DEAA mutant Na^+ channel. Similar relief-of-block behavior has been previously documented for many types of ions channels and blockers. For example, relief of block at high voltage has been observed for block of the squid axon K^+ channels by internal Na^+ (French and Wells, 1977; French and Shoukimas, 1985), block of acetylcholine-receptor channels by high concentrations of external acetylcholine (Sine and Steinbach, 1984), and block of anthrax toxin channels by large TAA^+ cations (Blaustein and Finkelstein, 1990a,b). The interesting feature here is that relief of block by such a large and bulky organic cation (diameter of $TPeA^+ \simeq 13.2$ Å) has not been previously reported for a cation-selective channel that has a rather narrow selectivity filter, on the order of 3×5 Å for the wild-type Na^+ channel (Hille, 1971, 1972; Sun et al., 1997).

One mechanism by which large molecules might pass through a small pore could involve physical deformation or a transient enlargement of the limiting region of the filter. To investigate this possibility, we tested the sensitivity of the relief-of-block phenomenon to toxins that block the Na^+ channel from the external side. The

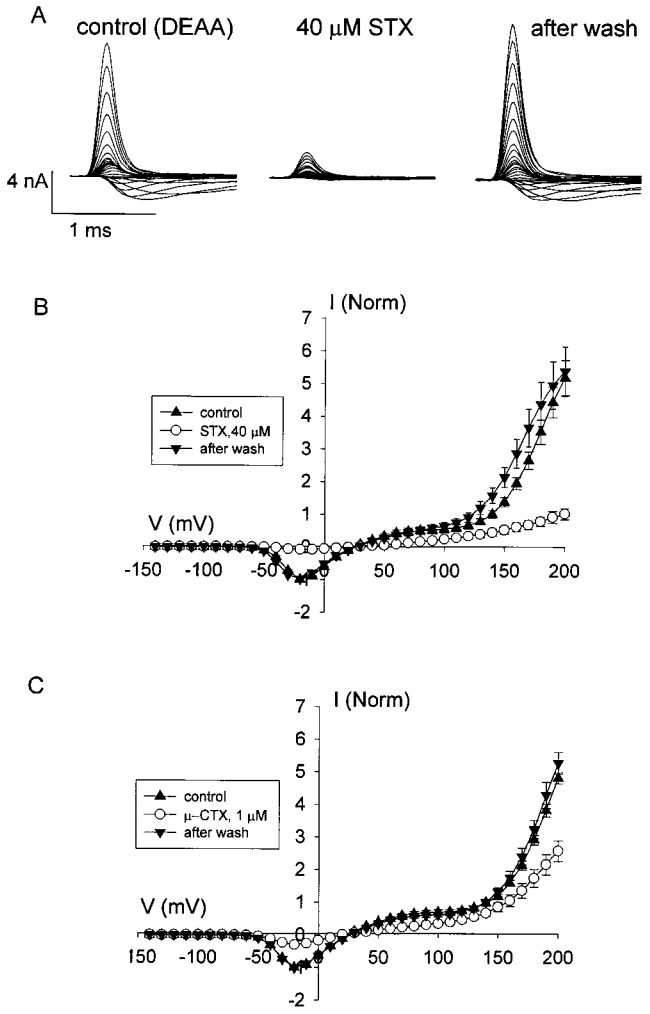

Figure 3. Sensitivity of currents of the DEAA mutant in the presence of internal TePA$^+$ to external Na$^+$ channel toxins. The voltage pulse protocol is the same as that of Fig. 2. (A) A typical set of current records from the same cell with standard Cs$^+$/Na$^+$ pipette solution plus 50 μM TPeA$^+$ in the pipette and standard Na$^+$ bath solution. Traces from one cell are shown in standard Na$^+$ bath solution (left), with 40 μM STX added to the bath solution (middle) and after wash back to standard bath solution minus STX (right). (B) I-V behavior of the DEAA mutant before and after the addition of 40 μM external STX, and after washout of STX. I-V data are normalized to the peak inward current of a given cell in the absence of STX. (C) I-V data for an experiment similar to that of A and B with sensitivity to 1 μM μ-conotoxin GIIIB (μ-CTX) tested instead of STX. Data points in B and C are the mean ± SEM for three to five cells.

experiments of Fig. 3 show that outward currents associated with relief of block by 50 μM internal TPeA$^+$ are partially inhibited by 40 μM STX and 1 μM μ-conotoxin GIIIB (μ-CTX). When bound to the Na$^+$ channel, these particular toxins interact with numerous residues in the outer mouth that are thought to be located near the entrance to the selectivity filter (Lipkind and Fozzard, 1994; Terlau et al., 1991). An irreversible change in structure of the outer pore would be likely to adversely impact molecular recognition between toxin and channel. The fact that these toxins reversibly inhibit outward currents associated with relief-of-block by TPeA$^+$ suggests that the outer mouth of the channel most probably retains its original conformation or quickly returns to it after this large molecule has passed though the channel. Relatively high concentrations of STX and μ-CTX are necessary for the experiments of Fig. 3 because the DEAA mutation itself lowers the affinity of such toxins relative to the wild-type channel (Sun et al., 1997). The results of Fig. 3 confirm that the relief-of-block phenomenon is mediated by STX- and μ-CTX–sensitive Na$^+$ channels. They also show that this is a robust phenomenon that does not irreversibly damage Na$^+$ channel function since the peak I-V curve taken with internal TPeA$^+$ is stable over the course of ≥30 min during continuous perfusion of the extracellular solution and multiple rounds of stimulation at high positive voltage. (As a finer point of interpretation, it is worth noting that the data of Fig. 3, B and C, suggest that STX and μ-CTX appear to be more effective at inhibiting inward current than outward current in the presence of internal TPeA$^+$. This may be due to trans effects of current flow or transient changes in toxin affinity associated with block or relief-of-block that will require further study to fully characterize.)

In studying relief of block by TPeA$^+$ in the DEAA mutant, we first hypothesized that voltage-driven permeation of this cation must be specifically related to a significant increase in the cutoff diameter of this mutant for organic cation permeation as previously found in molecular sieving studies (Sun et al., 1997). However, similar experiments with the wild-type μ1 Na$^+$ channel show that this is not the case. A comparison of normalized peak I-V curves taken in the absence and presence of 50 μM TPeA$^+$ (Fig. 4) confirm that internal TPeA$^+$ is a strong voltage-dependent blocker of the wild-type Na$^+$ channel. This is demonstrated by the sharp decrease in conductance in the low positive voltage range for I-V data collected with TPeA$^+$. The wild-type Na$^+$ channel also exhibits the relief-of-block phenomenon for TPeA$^+$ as recognized by a positive upward inflection of the peak I-V relation at high positive voltage. One clear difference in the behavior of the DEKA wild-type Na$^+$ channel and the DEAA mutant is the nonlinearity of control outward currents versus positive voltage for the wild-type channel (compare Figs. 4 A and 2 B). We first presumed that this inward rectification was due to strong Na$^+$ selectivity of the wild-type Na$^+$ channel and presence of a less permeable cation, Cs$^+$, in the pipette solution. However, additional experiments with the wild-type Na$^+$ channel using Na$^+$ as the only major cation in both the internal and external solutions suggest that inwardly rectifying I-V behavior of the wild-type channel at high positive voltages cannot solely be at-

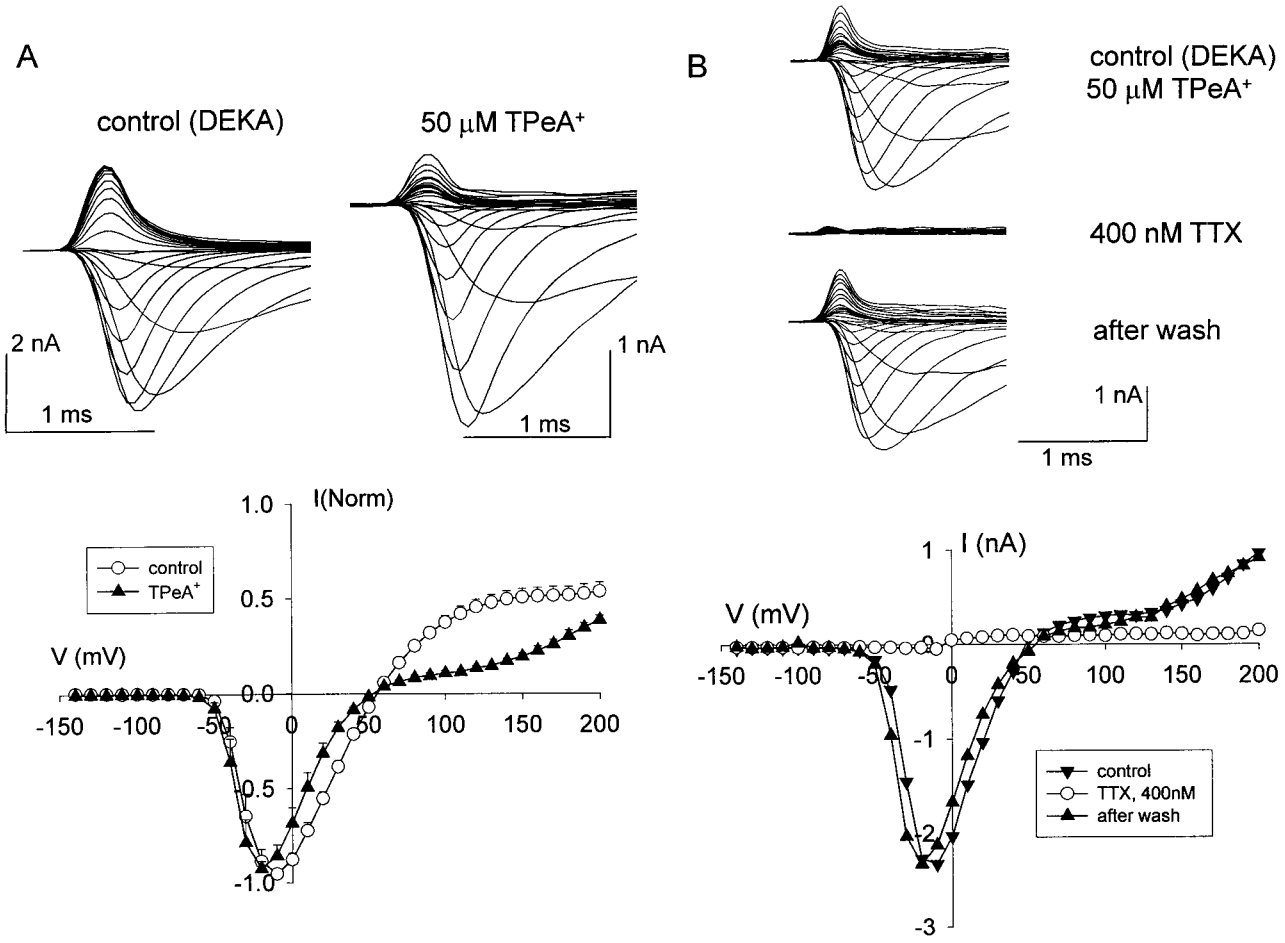

Figure 4. Block and relief-of-block by internal $TPeA^+$ as observed for the DEKA wild-type μ1 Na^+ channel. The voltage pulse protocol is the same as that of Fig. 2. (A) Typical current records with standard Cs^+/Na^+ pipette solution and standard Na^+ bath solution in the absence (left) and presence (right) of 50 μM $TPeA^+$ in the pipette solution. (Bottom) Peak I-V data in the absence and presence of 50 μM $TPeA^+$. Data points are normalized to the peak inward current for each condition and averaged as mean ± SEM of six to eight cells. (B) Effect of TTX on DEKA wild-type currents in the presence of internal $TPeA^+$. (Top) Typical current records from the same cell in standard Na^+ bath solution (top), with 400 nM TTX added to the bath solution (middle) and after washout of TTX (bottom). (Bottom) Corresponding I-V data.

tributed to internal Cs^+, Mg^{2+}, or HEPES (Huang and Moczydlowski, unpublished results). Rather, a major component of such inward rectification seems to be due to an endogenous blocking molecule that perfuses slowly from the cell to the pipette (data not shown). Characterization of this latter behavior is being pursued in separate studies and will not be further analyzed here. Regardless of this complication, the peak I-V relationship of the wild-type Na^+ channel in the presence of internal $TPeA^+$ shows an upward inflection in the positive voltage range that is qualitatively like that of the DEAA channel. The positive inflection in the I-V curve of the wild-type channel is also sensitive to 400 nM external TTX, another toxin that blocks in the external vesibule (Fig. 4 B). Thus, this unusual I-V behavior is likely to represent voltage-driven permeation of $TPeA^+$ through the wild-type channel.

The Relief-of-Block Phenomenon Is Enhanced for Long Chain TAA^+ Derivatives

The next question we addressed concerned the structural requirements of organic cations that favor the relief-of-block phenomenon. We tested the relative ability of the series of symmetrical TAA^+ cations to exhibit relief of block as judged by a positive inflection in the whole-cell peak I-V curve taken with various blockers in the pipette solution. Blockers ranging in size from TEA^+ to $TPeA^+$ were tested at concentrations at or above their reported blocking K_d at 0 mV for native heart Na^+ channels (O'Leary et al., 1994; O'Leary and Horn, 1994). Surprisingly, we found that relief of block is an exclusive feature of long-chain TAA^+ derivatives. Peak I-V data for the DEAA mutant with internal TEA^+ (50 mM) or TPA^+ (5 mM) essentially reflects pure voltage-dependent block, as indicated by the strong sup-

pression of outward current throughout the positive voltage range (Fig. 5, B and C). In contrast, TBA^+ (0.5 mM), $TPeA^+$ (50 μM), and $THexA^+$ (25 μM) exhibit clear evidence of relief of block indicated by an upward inflection of the I-V curve at high positive voltage (Fig. 5 B). Fig. 5 B (inset) shows that relief of block commences at lower positive voltages for the longest chain derivative, $THexA^+$, as compared with TBA^+. This implies that it is energetically easier to drive the larger $THexA^+$ cation through the channel than the smaller TBA^+ cation, a conclusion that is borne out in model simulations described later (see Fig. 9). A similar pattern seems to be followed by the wild-type DEKA channel, since I-V data for $TPeA^+$ and $THexA^+$ also exhibit an upward inflection at positive voltage, whereas smaller blockers do not show such an obvious upturn (Fig. 5 A). However, results for the wild-type channel are complicated by the presence of background or "endogenous" inward rectification that makes it more difficult to discern relief-of-block by simple inspection of peak-normalized I-V data. We also find that the lidocaine derivative, $QX\text{-}314^+$, does not exhibit relief-of-block as judged from the I-V behavior of either the wild-type channel (not shown) or the DEAA mutant (Fig. 5 B, inset, and

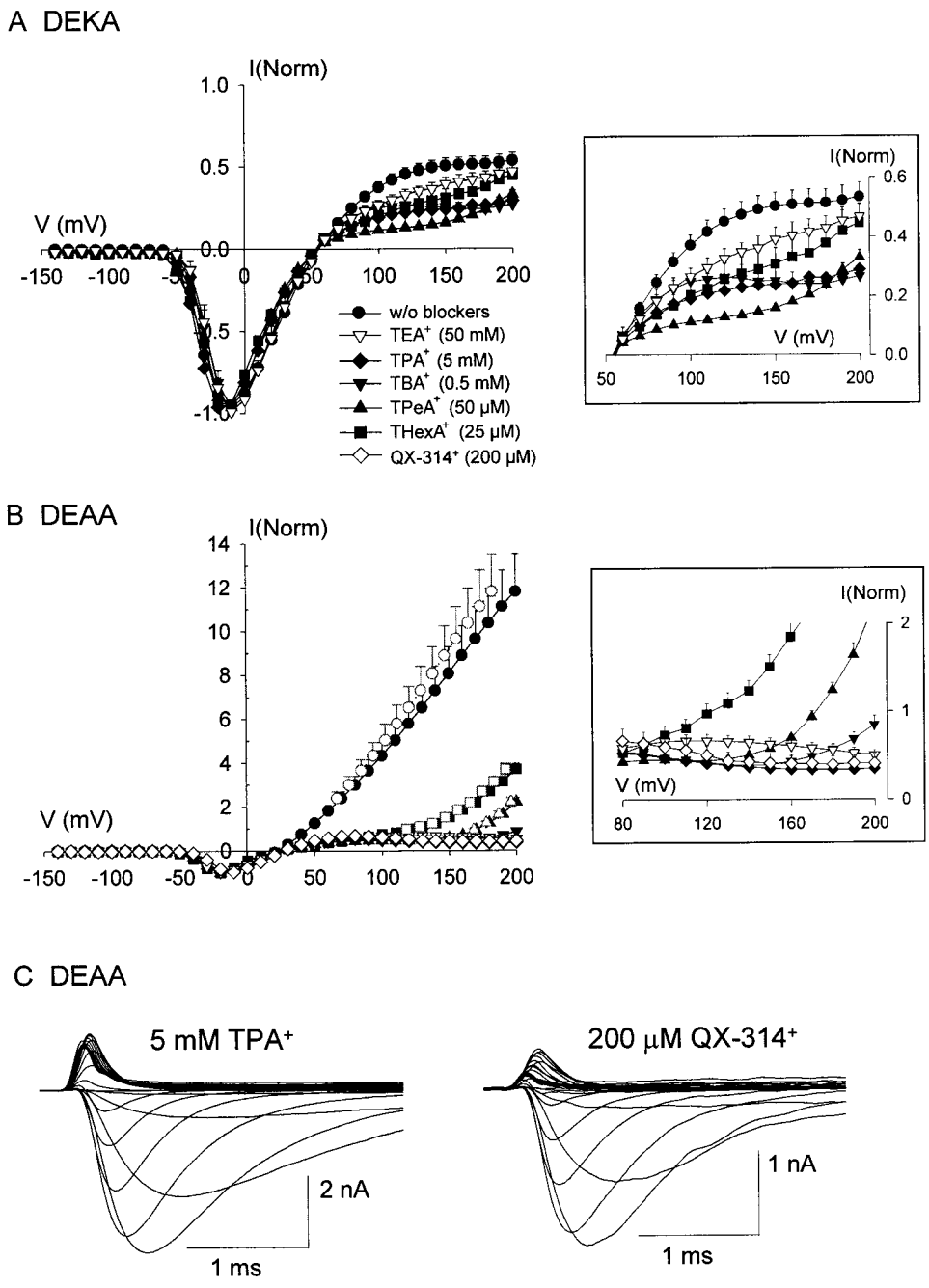

Figure 5. Test for relief-of-block by a series of TAA^+ cations and $QX\text{-}314^+$ in wild-type DEKA and mutant DEAA Na^+ channels. Except for TEA^+, currents were recorded using standard Na^+ bath solution and Cs^+/Na^+ pipette solution in the absence or presence of various test blockers in the pipette solution at the indicated concentrations. The pipette solution used to test internal TEA^+ block was 50 mM TEA-Cl, 73 mM CsF, 2 mM $MgCl_2$, 1.1 mM EGTA, 10 mM glucose, 20 mM Na-HEPES, pH 7.3 with CsOH. (A) Superimposed peak I-V data for the DEKA wild-type channel. Data points are normalized to the peak inward current for a given cell and averaged for each condition ± SEM of four to eight cells. (B) The same comparison as for A, plus results for $QX\text{-}314^+$, are shown for the DEAA mutant channel. Lightly shaded symbols to the left of data points for control with no blockers, $TPeA^+$, and $THexA^+$ are approximate corrections of applied voltage for series resistance error at large voltage steps. The inset (right) in A and B shows an expanded view of the same data in the positive voltage range. (C) Typical current records corresponding to data of B for the DEAA mutant with 5 mM TPA^+ and 200 μM $QX\text{-}314^+$ show a lack of blocking relief at high positive voltage.

C). In summary, the results of Fig. 5 indicate that voltage-dependent relief of block is enhanced with increasing length of *n*-alkyl chains for the series of symmetrical TAA^+ cations. The fact that QX-314$^+$ does not exhibit relief-of-block at +200 mV or less suggests that there are rather specific chemical structural requirements for voltage-driven permeation of quaternary ammonium cations through the external end of the pore.

Current–Voltage Behavior in the Presence of Internal $TPeA^+$ Depends on the Frequency of Stimulation

The binding of many local anesthetic drugs to an internal blocking site of voltage-gated Na^+ channels is known to exhibit use dependence, a phenomenon in which the occupancy of the site by the drug increases with the frequency of stimulation (Courtney, 1975; Hille, 1977; Hondeghem and Katzung, 1977). In the case of TAA^+ cations, O'Leary et al. (1994) found that TBA^+ and $TPeA^+$ exhibit use-dependent block of heart Na^+ channels when repetitively stimulated at a frequency of 1 Hz, whereas smaller TAA^+ derivatives do not. If the positive inflection of the peak I-V relation that we observe involves outward dissociation of $TPeA^+$ from the internal blocking site, one would expect that this phenomenon would also depend on the occupancy of the blocking site and the stimulation frequency.

Use-dependent block of Na^+ channels is traditionally monitored by a series of identical depolarizing voltage pulses delivered at various frequencies of repetitive stimulation. However, in the present case, we were interested in whether use dependence affects the shape of the peak I-V curve collected here by a series of increasingly positive voltage steps. To examine this possibility, we varied the rate at which consecutive points of the peak I-V relation are collected. The standard protocol for taking I-V data in this study used a waiting period of 0.5 s between consecutive voltage pulses, starting from −140 to +200 mV. This corresponds to a stimulation frequency of 2 Hz between successive I-V data points. Fig. 6 B shows that the shape of the peak I-V relation for outward current of the DEAA mutant exposed to 50 μM internal $TPeA^+$ depends on the rate of consecutive voltage pulses. At a low stimulation rate of one pulse every 10 s (0.1 Hz), the positive inflection of the outward I-V relation is rather shallow. As the stimulation rate is increased from 0.1 to 2 Hz, the plateau region of the I-V curve observed in the range of +50 to +150 mV is enhanced. This effect corresponds to stronger block that would be expected if a higher stimulation rate increases the occupancy of the blocking site by $TPeA^+$. At all tested frequencies, a positive inflection in the I-V curve is still observed in the high voltage range, but the transition from blocking behavior to relief-of-block is accentuated at higher stimulation frequency. This is consistent with the idea that the positive inflection in the I-V curve represents voltage-dependent exit of $TPeA^+$ from the blocked/inactivated state of the Na^+ channel that also occurs in the phenomenon of use-dependent block. Fig. 6 A shows that the wild-type Na^+ channel responds in a similar fashion to increasing stimulation frequency in this experiment; however, the relative enhancement of block in the positive voltage range is much less than that of the DEAA mutant. This implies that the blocking kinetics of $TPeA^+$ must differ for the wild-type versus mutant channel.

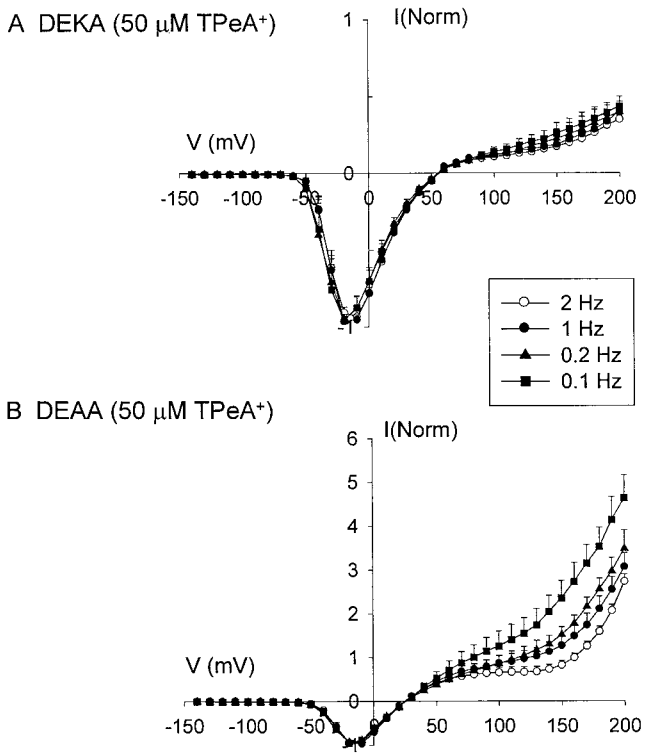

Figure 6. Test for use dependence of block and relief of block by $TPeA^+$. Currents were recorded using standard Na^+ bath solution and Cs^+/Na^+ pipette solution with 50 μM $TPeA^+$. (A) Superimposed peak I-V data for the DEKA wild-type channel. Whole-cell currents were recorded with a series of consecutive 10-ms voltage steps of +10 mV from a holding potential of −120 mV at intervals of 0.5 s (2 Hz), 1 s (1 Hz), 5 s (0.2 Hz), or 10 s (0.1 Hz) as indicated. Data points are normalized to the peak inward current for a given cell and expressed as the mean ± SEM of at least three cells. (B) The same protocol as in A is shown for the DEAA mutant channel. Each point is the mean ± SEM of at least four cells.

The DERA Mutant also Exhibits Relief of Block by $TPeA^+$

To further investigate how the amino acid residue at the K(III) position of the DEKA locus affects the relief-of-block phenomenon, we examined this behavior in a DERA mutant in which the Lys residue at this position is replaced by Arg. We previously showed that the DERA mutant of the μ1 Na^+ channel is nonselective toward Na^+ versus K^+ and does not support a macroscopically detectable inward Ca^{2+} current in *Xenopus* oocytes (Favre et al., 1996). Since a positively charged residue at the

K(III) position seems to function in preventing inward permeation of divalent cations, this led to the conclusion that the mechanism of exclusion of external Ca^{2+} involves a repulsive electrostatic interaction with the side chain of the K(III) residue. The question addressed here is whether a different positively charged residue in the selectivity filter such as Arg would prevent voltage-driven permeation of internal $TPeA^+$ through the channel.

We first confirmed that the DERA mutant is impermeable to external Ca^{2+} when expressed in HEK293 cells. This is shown by the experiment of Fig. 7 A in which replacement of extracellular Na^+ solution by Ca^{2+} solution results in a complete loss of inward current, a result that is quite similar to that obtained for the DERA mutant expressed in *Xenopus* oocytes (Favre et al., 1996).

We next tested whether the molecular sieving behavior of the DERA mutant is altered with respect to external organic cations. The wild-type μ1 Na^+ channel is impermeant to external MA^+, whereas this organic cation supports a sizeable inward current through the DEAA mutant that is 32% of the peak inward Na^+ current with a calculated permeability ratio of $P_{MA}/P_{Na} = 0.41 \pm 0.04$ (Sun et al., 1997). Fig. 7 B shows that external MA^+ is less permeant through the DERA channel than DEAA. MA^+ supports a very small inward current for DERA that is only ~8% of the peak inward Na^+ current and it has a calculated permeability ratio of $P_{MA}/P_{Na} = 0.28 \pm 0.01$ ($n = 4$). Thus, the permeability of external MA^+ through the DERA channel is intermediate between that of wild-type DEKA and the mutant DEAA channel. This indicates that a positively charged Arg residue at the K(III) position of the DEKA locus restricts the entry of a small organic cation more effectively than an Ala residue at this position, but Arg is less effective than the native Lys residue. This supports the previous conclusion that molecular sieving of organic cations is not a simple function of the charge and side-chain volume of residues at the DEKA locus (Sun et al., 1997).

Fig. 8 A shows the whole-cell peak I-V behavior up to +200 mV of the DERA mutant with 125 mM Cs^+ plus 20 mM Na^+ as the major internal cations. This mutant exhibits a much larger relative outward current than the wild-type DEKA channel under these conditions (compare Figs. 8 A and 5 A). However, the corresponding rel-

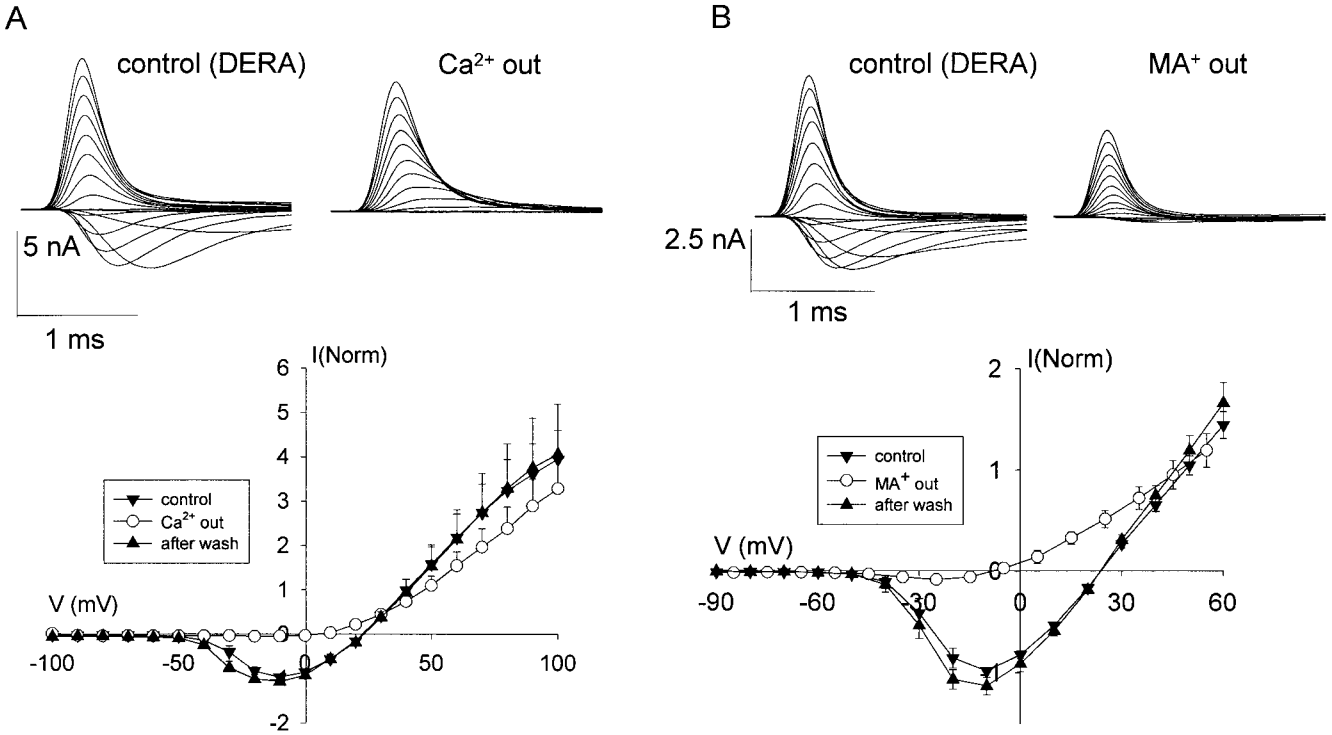

Figure 7. Test for permeation of Ca^{2+} and MA^+ through the DERA mutant channel. Whole-cell currents were recorded with a series of consecutive 10-ms voltage steps of +10 mV from a holding potential of −120 mV at intervals of 1 s. (A) External Ca^{2+} is impermeant. (Top) Typical records with standard Cs^+/Na^+ pipette solution and standard Na^+ bath solution (left) and after perfusion of the same cell (right) with Ca^{2+} bath solution (86 mM $CaCl_2$, 3 mM KCl, 2 mM $MgCl_2$, 10 mM glucose, 10 mM HEPES-Tris, pH 7.3). (Bottom) Peak I-V curves in control Na^+ bath solution, after replacement with Ca^{2+} bath solution, and again after wash with control Na^+ solution. (B) External MA^+ is weakly permeant. (Top) Typical currents before and after perfusion of the same cell with MA^+ bath solution (142 mM MA-Cl, 2 mM $MgCl_2$, 2 mM $CaCl_2$, 10 mM glucose, 10 mM HEPES-TMA, pH 7.3). (Bottom) Normalized peak I-V data in control Na^+ bath solution, after replacement with MA^+ bath solution, and again after wash with control Na^+ solution. Data points in A and B are normalized to the peak inward current of a given cell in the presence of control Na^+ bath solution and plotted as the mean of four cells ± SEM.

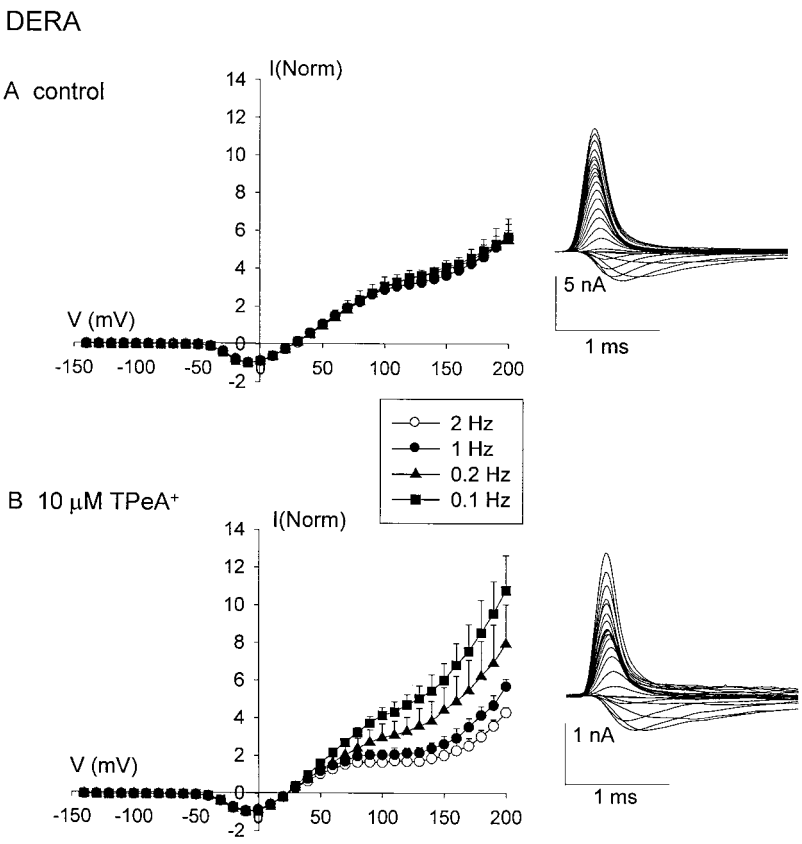

Figure 8. Test for use dependence of block and relief of block by $TPeA^+$ in the DERA mutant. Currents were recorded using standard Na^+ bath solution and Cs^+/Na^+ pipette solution without (A) and with (B) 10 mM $TPeA^+$ in the pipette solution. (A) Superimposed peak I-V data for the DERA mutant channel. Whole-cell currents were recorded with a series of consecutive 10-ms voltage steps of +10 mV from a holding potential of −120 mV at intervals of 0.5 s (2 Hz), 1 s (1 Hz), 5 s (0.2 Hz), or 10 s (0.1 Hz) as indicated. Data points are normalized to the peak inward current for a given cell and expressed as the mean ± SEM for three to five cells. (Right) Typical current records obtained at intervals of 0.5 s (2 Hz). (B) Results for the same protocol described in A with 10 μM $TPeA^+$ in the pipette.

ative outward conductance of the DEAA mutant is still about twice as large and more ohmic in nature than that of DERA (compare Figs. 2 B and 8 A). Therefore, the amino acid residue at the K(III) position of the DEKA locus seems to be an important determinant of I-V rectification behavior of outward current through the μ1 Na^+ channel. The peak I-V relation of the DERA mutant also exhibits a reproducible positive inflection in the vicinity of +140 mV in the absence of any added internal blockers (Fig. 8 A). We have not yet determined the basis of this interesting behavior, but we offer two possible explanations that require further investigation: (a) the Arg residue at the K(III) position of the DEKA locus may introduce or alter some kind of intrinsic rectification of the Na^+ channel pore with respect to alkali cations, and (b) the Lys(III)/Arg(III) residue controls the permeability of an endogenous blocking molecule.

The peak I-V behavior of the DERA mutant with 10 μM $TPeA^+$ in the internal solution is shown in Fig. 8 B. This data indicates that internal $TPeA^+$ blocks the DERA mutant in a use-dependent fashion as demonstrated by a marked enhancement of a plateau phase of the I-V curve in the range of +50 to +140 mV by increasing frequency of stimulation from 0.1 to 2 Hz. This behavior is rather similar to that of DEAA channel (compare Figs. 8 B and 6 B). There is also a sharp upward inflection of the I-V curve for DERA in the presence of internal 10 μM $TPeA^+$ at high positive voltage and at high stimulation frequency (Fig. 8 B). The lack of similar use dependence for the endogenous I-V inflection in the absence of internal $TPeA^+$ (Fig. 8 A) distinguishes this phenomenon from the $TPeA^+$ blocking effect and indicates that the DERA mutant supports significant relief of block by $TPeA^+$. Thus, the presence of an Arg residue at the K(III) position of the DEKA locus does not seem to seriously impede the ability of $TPeA^+$ to be driven outward through the selectivity filter at high voltage.

Relief-of-Block by TAA^+ Cations Can Be Simulated by a Simple Kinetic Model of a Permeant Blocker

To assess whether I-V behavior in the presence of large TAA^+ cations in the internal solution can be described by a mechanism based on voltage-dependent relief of block, we used a simple kinetic model to simulate this behavior for the DEAA mutant. This model is similar to one previously used by Sine and Steinbach (1984) to analyze external block and inward permeation of acetylcholine through acetylcholine-receptor channels. It is a simplification of the model of Woodhull (1973), originally used to describe the blocking effect of external and internal H^+ on the conductance of Na^+ channels. The model may be summarized by Scheme I.

$$B_{in} + O \underset{k_{-1}}{\overset{k_1[B]}{\rightleftharpoons}} O{\bullet}B \xrightarrow{k_{-2}} O + B_{out}$$

(SCHEME I)

In Scheme I, an internal blocker, B_{in}, reversibly binds to an internally accessible site in the open channel, O, with an equilibrium dissociation constant of $K_1 = k_{-1}/k_1$. Binding of B_{in} results in a nonconducting blocked state, O•B. Outward permeation of the blocker is governed by the k_{-2} rate constant, which leads to recovery of the open state and infinite dilution of the blocker in the external solution. Since outward current of the DEAA mutant exhibits nearly ohmic behavior in the absence of internal blocker, an expression for simulating peak whole-cell current for this channel as a function of voltage can be approximated by an ohmic conductance multiplied by the probability that the channel is opened by activation gating and the probability that the channel is not occupied by the internal blocker. Ohm's law can be used to describe channel conductance and a standard Boltzmann expression can be used to simulate the probability of channel activation as a function of voltage. The probability that the channel is not blocked can be computed by using the apparent blocker dissociation constant for Scheme I: $K_B = (k_{-1} + k_{-2})/k_1$. This relationship can be written as:

$$\begin{aligned} I = {} & [G_{max}(V - V_R)] \\ & \cdot \{1 + \exp[-q(V - V_{0.5})/A]\}^{-1} \\ & \cdot \{1 + [B_{in}]/K_B(V)\}^{-1} \end{aligned} \quad (1)$$

where G_{max} is the maximal conductance, V_R is the reversal potential, q is an effective gating charge for voltage activation, $V_{0.5}$ is the midpoint voltage of activation gating, A is a constant equal to RT/F, or 25.4 mV, and $[B_{in}]$ is the internal blocker concentration. It can be shown that $K_B(V)$ for Scheme I is equivalent to the product of the voltage-dependent equilibrium dissociation constant for internal block in the absence of an external permeation path, $K_1(V)$, times a term that contains the quantity, $R(V) = k_{-2}(V)/k_{-1}(V)$, which is the ratio of the rate constant of blocker dissociation to the external solution over that of the internal solution. These relationships and their voltage dependence can be expressed as:

$$\begin{aligned} K_B(V) &= K_1(V)[1 + R(V)] \\ K_1(V) &= K_1(0)\exp(-z\delta_1 V/A) \\ R(V) &= \frac{k_{-2}(0)}{k_{-1}(0)}\exp(z\delta_2 V/A) \end{aligned} \quad (2)$$

In Eq. 2, $K_1(0)$, $k_{-2}(0)$, and $k_{-1}(0)$ are the values of the respective equilibrium and rate constants at 0 mV, and z is the valence of the blocker (+1 for TAA^+). δ_1 is the summed fraction of electrical distance sensed by the blocker for the k_1 step plus the k_{-1} step, and δ_2 is the summed fraction of electrical distance attributed to the k_{-2} step plus the k_{-1} step. The latter use of summed electrical distances in this simplified model is used to reduce the number of free parameters for the purpose of data fitting.

By empirical testing, we found that parameters for fitting this model to the actual macroscopic I-V data are closely constrained since G_{max}, V_R, q, and $V_{0.5}$ are well defined by data points in the negative to low positive range, where blocking phenomena have only a small contribution. The behavior in the high positive voltage range is governed by $K_B(0)$ and δ_1, which determine current inhibition (block). Relief of inhibition at high voltage is governed by $R(0)$, the ratio of $k_{-2}(V)/k_{-1}(V)$ at 0 mV, and δ_2, the lumped electrical distance of the k_{-2} step plus the k_{-1} step. Fig. 9 shows that this model can readily simulate the unusual shape of macroscopic peak I-V curves of the DEAA channel in the presence of TBA^+, $TPeA^+$, and $THexA^+$. The average blocking parameters for fitting these data are summarized in Table I. The fitted values of $K_1(0)$ and δ_1 for TBA^+ and $TPeA^+$ are similar to those reported for internal block of the human heart Na^+ channel by these compounds in the voltage range less than +80 mV (O'Leary et al., 1994; O'Leary and Horn, 1994): $K_1(0) = 0.48$ mM for TBA^+ and 0.098 mM for $TPeA^+$; $\delta_1 = 0.46$ for TBA^+ and 0.41 for $TPeA^+$. The fitted values of $R(0)$ listed in Table I indicate that the k_{-2} rate of outward permeation for TBA^+ and $TPeA^+$ only has to be $\sim$2–3 $\times 10^{-4}$ of the k_{-1} rate for dissociation of these blockers back to the inside compartment to simulate the kind of blocking relief observed in this system. Table I also shows that the enhanced relief of block observed for $THexA^+$ can be explained by a 100-fold increase in the value of $R(0)$ for this particular molecule. This implies that $THexA^+$ is able to exit through the channel to the outside much more readily that TBA^+ and $TPeA^+$. Table I also shows that large values of δ_2 $\geq$1.0 are required to simulate the steep voltage dependence of the relief of block observed at high positive voltage. This indicates that additional charge-dependent processes besides the simple interaction of a single cation with a site in the transmembrane electric field are involved in generating this phenomenon.

We must also caution that these simulations have certain quantitative limitations. The model assumes that the measured peak Na^+ currents are proportional to the steady state interaction of the blockers with the open channel. This does not take into account the shortening of the apparent rate of channel inactivation that is evident in the current traces with large TAA^+ cations. This effect is especially dramatic at high positive voltage for current records in the presence of TBA^+ shown in Fig. 9. The simulations also do not consider the use or frequency dependence inherent in collecting

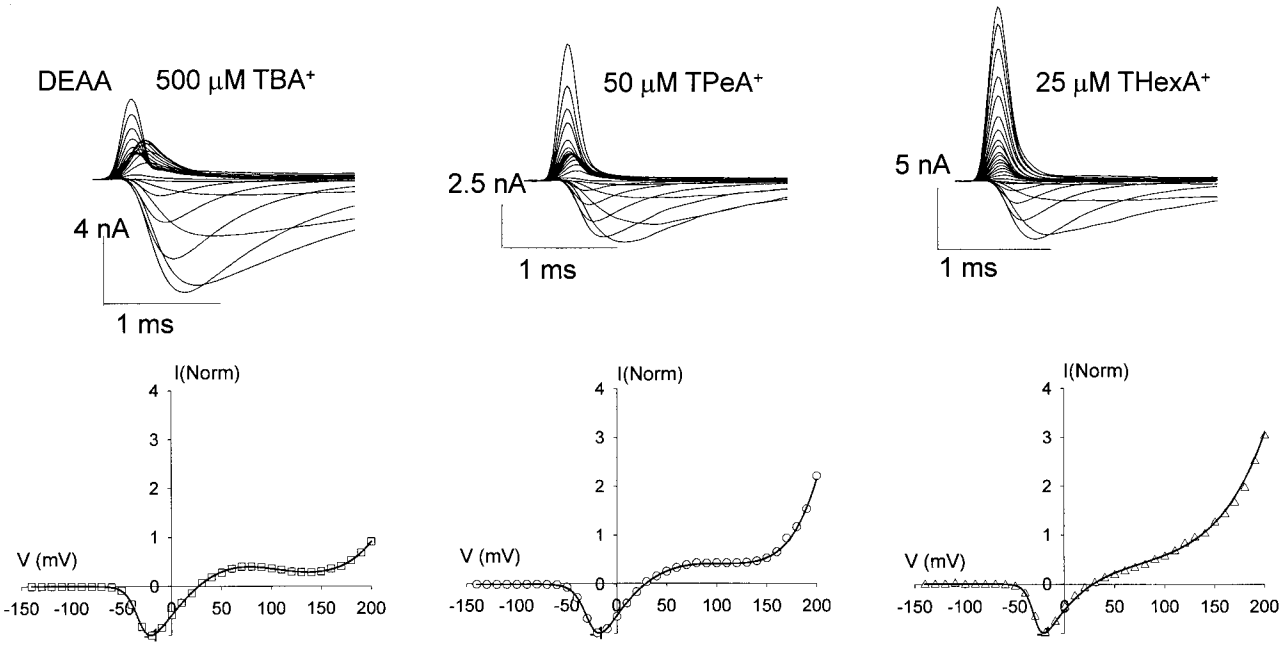

Figure 9. Comparison of relief of block by TBA^+, $TPeA^+$, and $THexA^+$ in the DEAA mutant channel and simulation of this phenomenon by a simple kinetic model of a permeant blocker. (Top) Typical current records with Na^+ bath solution and Cs^+/Na^+ pipette solution with 500 μM TBA^+ (left), 50 μM $TPeA^+$ (middle), or 25 μM $THexA^+$ (right). The voltage pulse protocol is the same as that described in Fig. 2. (Bottom) Normalized peak I-V data from the corresponding experiment at the top. Solid lines through the data points correspond to a fit to the kinetic model of Scheme I. Averaged parameters used to fit the data are summarized in Table I.

the I-V data of Fig. 9. Despite these deficiencies, the modeling exercise shows that I-V data for the DEAA mutant Na^+ channel are closely mimicked by a simple theory of voltage-dependent relief of block. Corrections to the model to account for kinetic effects will change absolute estimates of the blocking parameters, but will not affect the central conclusion that this process represents voltage-driven permeation of large organic cations.

DISCUSSION

The primary goal of this study was to determine whether the K(III) residue of the Na^+ channel DEKA locus plays a role in controlling intracellular blocking interactions of TAA^+s. In the course of this investigation, we found that the rectification behavior of outward current is strongly affected by two different mutations of the K(III) residue. We also observed an unexpected phenomenon involving voltage-dependent relief of block by large TAA^+ cations.

The first conclusion is that substitution of a butylammonium group with a methyl group that is effectively achieved by mutation of Lys(III) to Ala(III) in the DEAA mutant increases the cutoff diameter for molecular sieving (Sun et al., 1997), but does not simply allow large organic cations to freely carry current in both directions. This point is demonstrated by marked asymmetry in the permeation of small TAA^+ cations such as TMA^+ and TEA^+ (Fig. 1) and the ability of $QX\text{-}314^+$ and TAA^+s larger than TMA^+ to block outward $Cs^+/$

TABLE I

Parameters obtained by Fitting Peak I-V Relations of the DEAA Mutant Na^+ Channel in the Presence of Intracellular TAA^+ Cations to a Simple Model of Voltage-dependent Relief of Block

TAA^+ cation	$K_1(0)$	δ1	R(0)	δ2
	mM			
TBA^+ (500 μM)	1.2 ± 0.1 (5)	0.64 ± 0.02	$3.0 \pm 1.2 \times 10^{-4}$	1.35 ± 0.08
$TPeA^+$ (10 μM)	0.037 ± 0.015 (5)	0.38 ± 0.03	$1.7 \pm 1.7 \times 10^{-4}$	1.81 ± 0.09
$TPeA^+$ (50 μM)	0.110 ± 0.026 (5)	0.52 ± 0.04	$2.4 \pm 0.9 \times 10^{-4}$	1.48 ± 0.05
$THexA^+$ (25 μM)	0.023 ± 0.01 (7)	0.45 ± 0.07	$3.1 \pm 1.5 \times 10^{-2}$	0.99 ± 0.09

All values are means ± SEM of fitting results for the number of data sets given in parenthesis after the value of $K_1(0)$. Peak I-V data sets such as those shown in Fig. 9 were fit to Eqs. 1 and 2 derived for Scheme I, with parameters defined in the text. The concentration of the particular TAA^+ blocker used in the pipette solution for each condition is shown in parenthesis after the TAA^+ cation.

Na^+ current in a voltage-dependent manner (Fig. 5 B). At voltages less than +100 mV, inhibition of outward macroscopic current of the DEAA mutant by large TAA^+ molecules is similar to previously described intracellular blocking behavior of native Na^+ channels by various local anesthetic-type agents. For example, voltage-dependent block by TEA^+, TPA^+, TBA^+ and $TPeA^+$ illustrated here by the data of Fig. 5 B and the parameters of Table I is reminiscent of previous observations that larger, more hydrophobic alkylammonium derivatives generally have higher affinity than TMA^+ and TEA^+, (Moczydlowski et al., 1986; Wang et al., 1991; O'Leary and Horn, 1994) and that this internal blocking site typically exhibits a δ in the range 0.4–0.7 based on the Woodhull (1973) blocking model. The results of Fig. 6 B demonstrate that use-dependent behavior of internal $TPeA^+$ like that previously described for a wild-type heart Na^+ channel (O'Leary et al., 1994) is also present in the DEAA mutant. Thus, the internal blocking site for hydrophobic organic cations is functionally preserved in the DEAA mutant. In mechanistic terms, substitution of the K(III) residue with Ala does not simply correspond to the removal of an energy barrier at an impassable location in the pore that controls voltage-dependent block by internal TAA^+s.

An interesting new feature of the DEAA channel described here is that whole-cell current carried by internal alkali cations (Cs^+, Na^+) in the absence of other added blockers is nearly ohmic at positive voltages up to +200 mV (e.g., Fig. 5 B). This stands in strong contrast to inwardly rectifying or sublinear I-V behavior of the wild-type DEKA channel in this voltage range (e.g., Fig. 5 A) recorded under the same conditions with Na^+ outside and Cs^+ inside. This feature of the DEAA mutant makes it easier to recognize the dramatic relief of block by large TAA^+ cations at voltages greater than +140 mV (e.g., Fig. 2 B). The wild-type DEKA channel also apparently exhibits a similar phenomenon (Fig. 4), but it is more difficult to analyze because of the background inward rectification. In this respect, a second conclusion of our study is that the K(III) residue of the DEKA locus controls the rectification behavior of outward macroscopic current of the μ1 Na^+ channel expressed in HEK293 cells. The outward I-V relation of the DERA mutant with the Lys(III) to Arg substitution is more linear than the wild-type DEKA channel, but a distinctive negative inflection in the I-V curve of the DERA mutant seen with Cs^+/Na^+ pipette solution (Fig. 8 A) further establishes that the particular residue at the K(III) position is a major determinant of current rectification.

The mechanism underlying the latter current inflection of the DERA channel and the sublinear I-V behavior of the wild-type channel is presently undetermined. However, our results provide clues that may help in its elucidation. Since block by various internal organic cations produces sublinear I-V behavior for the DEAA mutant, and certain mutations of the K(III) residue enhance permeation of organic cations, an obvious possibility is that an endogenous internal blocking molecule is partially responsible for inward rectification of the wild-type channel. As mentioned in results, our initial experiments suggest that Mg^{2+}, Cs^+, or HEPES, which are all present in the standard pipette solution, are not the only molecular species that may be responsible for this effect. At present, we suspect that other cellular cations such as polyamines may be involved in the endogenous rectification of wild-type Na^+ channels, since polyamine block has been found to underlie inward rectification behavior of other classes of ion channels (Williams, 1997).

The third conclusion of this work is that voltage-dependent relief of block by the series of symmetrical TAA^+ cations is facilitated by increasing length of *n*-alkyl chains. Where this phenomenon is easiest to study, in the DEAA mutant, there is little hint of relief of internal block due to TEA^+, TPA^+, or $QX314^+$ by positive voltage up to +200 mV (Fig. 5, B and C). In contrast, a distinct upturn in the I-V curve appears to commence at progressively lower voltages for the series, TBA^+, $TPeA^+$, and $THexA^+$ (Figs. 5 B and 9). As demonstrated by the modeling exercise of Fig. 9, this behavior is consistent with voltage-driven permeation of large TAA^+ cations to the outside of the channel. The structure–activity dependence of this effect implies that the permeation process is facilitated by hydrophobic interactions. However, this is a rather unusual type of hydrophobic interaction. The increase in hydrophobicity with increasing *n*-alkyl chain length of symmetrical TAA^+ cations is accompanied by a proportional increase in molecular diameter, which would ordinarily be expected to inhibit permeation through a fixed-diameter pore in the usual manner of molecular sieving. Using energy-minimized molecular models of TAA^+ cations (Hyperchem software from Hypercube), we find that the molecular diameter of these molecules increases by $\sim$2 Å per symmetrical addition of a methylene group, as in the series: TMA^+ (6.0 Å), TEA^+ (8.2 Å), TPA^+ (9.8 Å), TBA^+ (11.6 Å), $TPeA^+$ (13.2 Å), and $THexA^+$ (15.2 Å), with the measured diameter given in parenthesis. The latter measurements are also in accord with an independent molecular dynamics analysis of the conformations and size of TAA^+ cations in the absence of solvent (O'Leary et al., 1994). Thus, the basic question posed by this phenomenon is: How do long *n*-alkyl chains of TAA^+ molecules facilitate movement of these blockers through a protein pore that has an effective cutoff size of 3×5 Å (Hille, 1971, 1972) for the wild-type Na^+ channel and an external cutoff diameter of $\sim$8.2 Å (Sun et al., 1997) for the DEAA mutant?

Similar questions have been contemplated previously in the literature. In the case of inhibition of outward

K^+ current through squid axon delayed-rectifier K^+ channels, block by both internal Na^+ and Cs^+ exhibits steeply voltage-dependent relief when external K^+ concentration is low (French and Wells, 1977; French and Shoukimas, 1985). In pondering the basis for this effect, the latter authors suggested that energy supplied by high voltage could be sufficient to permit dehydrated Na^+ ions to move through the K^+-selective region of the channel, by a process that is energetically prohibitive under normal conditions. As another possibility, they speculated that the structure of the channel could be physically distorted under the stress of high voltage acting upon impermeant ions in the pore. In a different study of a sarcoplasmic reticulum K^+ channel using a series of bis-quaternary ammonium blockers (bis-QA^+) of increasing *n*-alkyl chain length, Miller (1982) observed an anomalous increase in the apparent voltage dependence of block by the longest bis-QA^+ molecules. He suggested that this could be explained by the binding of the blocker molecule in a "bent-over" conformation, such that this channel might simultaneously accommodate two charges of a 10-carbon bis-QA^+ molecule folded in a strained conformation. As applied to the present situation, these mechanisms require that either the narrow filter region of the Na^+ channel protein undergo deformation by a transient enlargement of the pore aperture, or the chemical conformation of the TAA^+ molecule physically contract to allow such a molecule to squeeze through the outer end of the pore and exit to the outside. Both of these mechanisms seem unlikely to fully explain the phenomenon encountered here. If the Na^+ channel protein is able to transiently deform to produce a wider pore, it is not clear why this should occur more readily for larger molecules such as $TPeA^+$ and not to any measurable extent for TEA^+ or TPA^+. Likewise, strained conformations of $TPeA^+$ that can be achieved by rotation about carbon–carbon bonds of *n*-alkyl chains cannot physically produce a structure as compact as TEA^+. So these two mechanisms do not explain why small TAA^+ cations are inhibited from permeating through the channel under duress of high voltage, whereas the permeation of large TAA^+ cations is facilitated.

One mechanism that may account for the observed preference for large TAA^+ molecules can be considered in reference to the molecular graphics illustration of Fig. 10. For the sake of discussion, this figure shows space-filling models of the KcsA K^+ channel, TEA^+, and $THexA^+$ at the same scale. The image on the left is a model of the KcsA structure with the four subunits alternately colored red and yellow. For orientation, Tyr82, a residue that constitutes an external aromatic binding site for TEA^+ in related K^+ channels (Heginbotham and MacKinnon, 1992) is colored blue. The view is looking down upon the external membrane surface of the protein along the central pore axis. In this orientation, the diameter of the whole KcsA tetramer measures 54 Å. Three K^+ ions and a water molecule in the pore have been removed from the structure to show the limiting diameter of the pore at the outer selectivity filter. The images on the right are molecular models of TEA^+ at the top and $THexA^+$ on the bottom. Each horizontal row shows two views (TEA^+) or possible conformations ($THexA^+$) of the same molecule. The view on the left is meant to emphasize the tetrahedral orientation of the alkyl chains. The view on the right shows a particular orientation with each of the *n*-alkyl chains located at a 90° planar rotation around the central nitrogen atom. In this fashion, four *n*-alkyl chains surrounding the central tetrahedral nitrogen of a TAA^+ molecule can be aligned with the four subunit interfaces of a tetrameric (KcsA) or pseudotetrameric (Na^+ channel) channel protein. We suggest that large TAA^+ cations that originally enter such a channel through an internal vestibule may diffuse across the narrow filter region to the outside by forming an alignment and inter-digitation of all four *n*-alkyl chains between the four protein subunit interfaces. Since the subunit interfaces are primarily hydrophobic contact surfaces, longer *n*-alkyl chains would have a greater propensity to partition into this environment (i.e., a stronger hydrophobic interaction energy) than shorter *n*-alkyl chains. Thus, this mechanism would naturally explain why large symmetrical TAA^+ molecules are more readily subject to relief-of-block under inducement of high voltage, whereas short TAA^+s are seemingly impervious to this driving force. A similar subunit hypothesis was previously proposed in reference to interactions of TAA^+ cations with squid axon K^+ channels (French and Shoukimas, 1981) and monazomycin channels (Heyer et al., 1976).

Although the illustration of Fig. 10 is based on the crystal structure of a K^+ channel protein, the pore domains of voltage-gated Na^+ and Ca^{2+} channels are likely to have a similar structure since they belong to a superfamily of channel proteins consisting of evolutionarily related sequences (Jan and Jan, 1990; Pongs et al., 1988). In particular, intersubunit interfaces of K^+ channels would correspond to pseudosubunit interfaces of Na^+ and Ca^{2+} channels since these latter proteins are actually composed of a single α subunit that contains four internally homologous domains, I, II, III, and IV. In any case, the molecular cutoff diameter of the selectivity filter of native Na^+ channels (3×5 Å) is only slightly larger than that of K^+ channels (3 Å). Fig. 10 is thus a reasonable representation of the physical limitations that must underlie the improbability of electrodiffusion of large TAA^+s through the Na^+ channel pore. One implication of this subunit interface hypothesis is that K^+ and Ca^{2+} channels may also exhibit relief

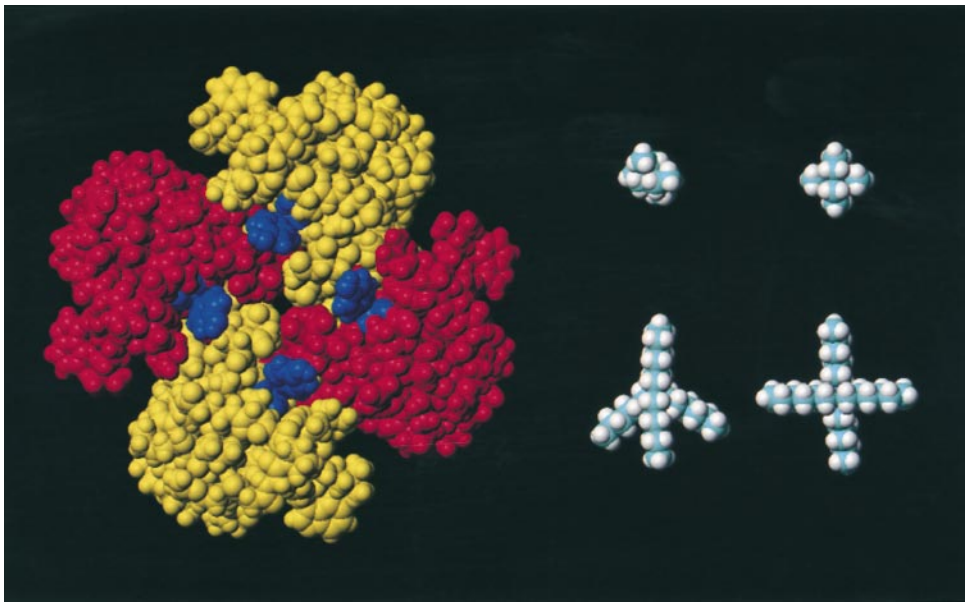

Figure 10. Space-filling models of the structure of the KcsA K^+ channel and two different TAA^+ cations at the same scale. The extracellular face of KcsA is shown with the four subunits alternately colored red and yellow. The extracellular residue, Tyr82, of KcsA is colored blue for reference. On the right, molecular models of TEA^+ (top) and $THexA^+$ (bottom) are shown in two different orientations (TEA^+) or conformations ($THexA^+$). This figure was prepared with WebLab ViewerPro software from Molecular Simulations Inc. using a crystal structure of KcsA (Doyle et al., 1998) taken from the Brookhaven protein data base (entry number 1BL8).

of block by molecules such as $TPeA^+$ at sufficiently high voltages. On the other hand, since the selectivity filter of Na^+ and Ca^{2+} channels is based on the DEKA/EEEE signature motif of charged residues, specific structural features of these two channel subfamilies may be required for permeation of large TAA^+s.

Another implication of this work is that the relief-of-block phenomenon ought to be useful for probing the mechanism of Na^+ channel gating and the interactions of local anesthetic drugs. In the case of local anesthestics, Hille (1977) postulated that such drugs could bind and unbind from native Na^+ channels by hydrophilic and hydrophobic pathways. This argument was put forward as a way to explain the complex kinetics of a variety of charged and uncharged molecules of different polarity that interact with closed, open, and inactivated states of the channel. To explain how uncharged hydrophobic drugs exhibit better access to closed states of the channel than charged molecules or to explain how bound drug molecules can escape from closed states of the channel, it was proposed that hydrophobic drugs may enter or leave the blocking site by diffusing through the channel wall from/to the hydrophobic membrane rather than being restricted to routes of entry and exit through the internal aqueous pore. In this study, we found a class of molecules that can apparently be driven through the pore more readily by virtue of hydrophobic interactions. Our subunit interface hypothesis is based on a similar idea as the "hydrophobic pathway" of local anesthetic action. If hydrophobic alkyl chains are able to partition into the subunit interfaces of Na^+ channels, then the uncharged forms of local anesthetics such as lidocaine may also use these interfaces as routes of diffusional access.

The notion that small molecules can enter cavities buried within the hydrophobic core of proteins by diffusing from the external solution is actually supported by a considerable body of evidence, mostly obtained from physical studies of soluble proteins. For example, fluorescence quenching and hydrogen exchange studies show that aromatic amino acid side chains and hydrogen atoms of peptide backbone amide groups buried in the interior of many proteins are accessible to collision and reaction with small molecules such as O_2, I^-, acrylamide, and H_2O at relatively rapid rates of diffusion (Creighton, 1983). Similarly, benzene and indole have been found to rapidly bind to a buried cavity in lysozyme with bimolecular association rates that are only a few orders of magnitude lower than the solution limit (Feher et al., 1996). The mechanism by which these kinds of small molecules gain access to the interior of protein cores is thought to involve penetration of the protein surface and subsequent diffusion along transient channels or pathways created by mobile defects or local unfolding of secondary structures that arise in the course of protein structural fluctuations (Feher et al., 1996). In channel proteins such as KcsA or voltage-gated Na^+ channels, interfaces between subunits, pseudosubunits, and packed transmembrane helices are obvious candidates for locations that may give rise to transient crevices in the protein structure that could facilitate the entry of small organic molecules.

If this interpretation is correct, the relief-of-block phenomenon may provide a new tool to monitor and investigate the interactions of drug molecules with subunit interfaces of the Na^+ channel. One approach would be to further examine the detailed structural requirements of organic cations for voltage-dependent relief of block. In this regard, it is interesting that $QX\text{-}314^+$ does not exhibit significant relief of block in the assay described

here (Fig. 5, B and C). This molecule has been previously observed to block the cardiac isoform of Na^+ channels from the outside of cells more readily than brain or muscle isoforms of Na^+ channels (Qu et al., 1995; Sunami et al., 1997). Since this latter effect has been proposed to occur by diffusion of QX-314^+ through the external Na^+ channel pore to an internal site (Qu et al., 1995; Sunami et al., 1997), it would be interesting to test whether voltage-driven relief of TAA^+ or $QX314^+$ block also varies among heart, brain, and muscle isoforms of Na^+ channels. The fact that significant voltage-driven relief of block by intracellular QX-314 is not observed for the DEAA mutant suggests that electrodiffusion of this molecule directly through the aqueous pore is a very unfavorable process. Other access routes, such as hydrophobic pseudosubunit interfaces, may have to be considered to explain such phenomena. Finally, since the DEAA mutant can be used to monitor the mobility of large TAA^+ molecules through entire permeation pathway of the Na^+ channel, it would be interesting to examine the differential accessibility of closed, open, and inactivated gating states of the channel to this process. Such studies may be helpful in refining our knowledge of the detailed conformational changes of the pore that occur in normal gating.

This research was supported by a grant from the National Institute of General Medical Sciences of the National Institutes of Health (GM-51172 to E. Moczydlowski).

Submitted: 14 December 1999
Revised: 17 February 2000
Accepted: 22 February 2000

REFERENCES

Armstrong, C.M. 1992. Voltage-dependent ion channels and their gating. *Physiol. Rev.* 72:S5–S13.

Armstrong, C.M., and L. Binstock. 1965. Anomalous rectification in the squid giant axon injected with tetraethylammonium chloride. *J. Gen. Physiol.* 48:859.

Armstrong, C.M., and W.F. Gilly. 1992. Access resistance and space clamp problems associated with whole-cell patch clamping. *Methods Enzymol.* 207:100–122.

Blaustein, R.O., and A. Finkelstein. 1990a. Voltage-dependent block of anthrax toxin channels in planar bilayer membranes by symmetric tetraalkylammonium ions: effects on macroscopic conductance. *J. Gen. Physiol.* 96:905–919.

Blaustein, R.O., and A. Finkelstein. 1990b. Voltage-dependent block of anthrax toxin channels in planar phospholipid bilayer membranes by symmetric tetraalkylammonium ions: single-channel analysis. *J. Gen. Physiol.* 96:921–942.

Choi, K.L., C. Mossman, J. Aube, and G. Yellen. 1993. The internal quaternary ammonium receptor of *Shaker* potassium channels. *Neuron*. 10:533–541.

Courtney, K.R. 1975. Mechanism of frequency-dependent inhibition of sodium currents in frog myelinated nerve by the lidocaine derivative GEA 968. *J. Pharmacol. Exp. Ther.* 195:225–236.

Creighton, T.E. 1983. Proteins: Structures and Molecular Principles. W.H. Freeman and Co., New York, NY. 515 pp.

Doyle, D.A., J.M. Cabral, R.A. Pfuetzner, A. Kuo, J.M. Gulbis, S.L. Cohen, B.T. Chait, and R. MacKinnon. 1998. The structure of the potassium channel: molecular basis of K^+ conduction and selectivity. *Science.* 280:69–77.

Favre, I., E. Moczydlowski, and L. Schild. 1996. On the structural basis for ionic selectivity among Na^+, K^+, and Ca^{2+} in the voltage-gated sodium channel. *Biophys. J.* 71:3110–3125.

Feher, V.A., E.P. Baldwin, and F.W. Dahlquist. 1996. Access of ligands to cavities within the core of a protein is rapid. *Nat. Struct. Biol.* 3:516–521.

French, R.J., and J.J. Shoukimas. 1981. Blockage of squid axon potassium conductance by internal tetra-*N*-alkylammonium ions of various sizes. *Biophys. J.* 34:271–291.

French, R.J., and J.J. Shoukimas. 1985. An ion's eye view of the potassium channel: the structure of the permeation pathway as sensed by a variety of blocking ions. *J. Gen. Physiol.* 85:669–698.

French, R.J., and J.B. Wells. 1977. Sodium ions as blocking agents and charge carriers in the potassium channel of the squid giant axon. *J. Gen. Physiol.* 70:707–724.

French, R.J., G. Zamponi, and I.E. Sierralta. 1998. Molecular and kinetic determinants of local anesthetic action on sodium channels. *Toxicol. Lett.* 100–101:247–254.

Gingrich, K.J., D. Beardsley, and D.T. Yue. 1993. Ultra-deep blockade of Na^+ channels by a quaternary ammonium ion: catalyis by a transition-intermediate state? *J. Physiol.* 471:319–341.

Heginbotham, L., Z. Lu, T. Abramson, and R. MacKinnon. 1994. Mutations in the K^+ channel signature sequence. *Biophys. J.* 66: 1061–1067.

Heginbotham, L., and R. MacKinnon. 1992. The aromatic binding site for tetraethylammonium ion on potassium channels. *Neuron*. 8:483–491.

Heinemann, S.H., H. Terlau, W. Stühmer, K. Imoto, and S. Numa. 1992. Calcium channel characteristics conferred on the sodium channel by single mutations. *Nature.* 356:441–443.

Heyer, E.J., R.U. Muller, and A. Finkelstein. 1976. Inactivation of monazomycin-induced voltage-dependent conductance in thin lipid membranes. I. Inactivation produced by long chain quaternary ammonium ions. *J. Gen. Physiol.* 67:703–729.

Hille, B. 1967. The selective inhibition of delayed potassium currents in nerve by tetraethylammonium ion. *J. Gen. Physiol.* 50: 1287–1302.

Hille, B. 1971. The permeability of the sodium channel to organic cations in myelinated nerve. *J. Gen. Physiol.* 58:599–619.

Hille, B. 1972. The permeability of the sodium channel to metal cations in myelinated nerve. *J. Gen. Physiol.* 59:637–658.

Hille, B. 1977. Local anesthetics: hydrophilic and hydrophobic pathways for the drug-receptor reaction. *J. Gen. Physiol.* 69:497–515.

Hille, B. 1992. Ionic Channels of Excitable Membranes. 2nd ed. Sinauer Associates, Inc., Sunderland, MA. 607 pp.

Hondeghem, L.M., and B.G. Katzung. 1977. Time- and voltage-dependent interactions of antiarrhythmic drugs with cardiac sodium channels. *Biochim. Biophys. Acta.* 472:373–398.

Jan, L.Y., and Y.N. Jan. 1990. A superfamily of ion channels. *Nature.* 345:672.

Kavanaugh, M.P., M.D. Varnum, P.B. Osborne, M.J. Christie, A.E. Busch, J.P. Adelman, and R.A. North. 1991. Interaction between tetraethylammonium and amino acid residues in the pore of cloned voltage-dependent potassium channels. *J. Biol. Chem.* 266: 7583–7587.

Lipkind, G.M., and H.A. Fozzard. 1994. A structural model of the tetrodotoxin and saxitoxin binding site of the Na^+ channel. *Biophys. J.* 66:1–13.

MacKinnon, R. 1995. Pore loops: an emerging theme in ion channel structure. *Neuron* 14:889–892.

MacKinnon, R., and G. Yellen. 1990. Mutations affecting TEA

blockade and ion permeation in voltage-activated K^+ channels. *Science.* 250:276–279.

Marty, A., and E. Neher. 1995. Tight-seal whole-cell recording. *In* Single-Channel Recording. B. Sakman and E. Neher, editors. Plenum Publishing Corp., New York, NY. 31–52.

Miller, C. 1982. Bis-quaternary ammonium blockers as structural probes of the sarcoplasmic reticulum K^+ channel. *J. Gen. Physiol.* 79:869–891.

Moczydlowski, E. 1998. Chemical basis for alkali cation selectivity in potassium channel proteins. *Chem. Biol. (Lond.)* 5:R291–R301.

Moczydlowski, E., A. Uehara, and S. Hall. 1986. Blocking pharmacology of batrachotoxin-activated sodium channels. *In* Ion Channel Reconstitution. C. Miller, editor. Plenum Publishing Corp., New York, NY. 405–428.

O'Leary, M.E., and R. Horn. 1994. Internal block of human heart sodium channels by symmetrical tetra-alkylammoniums. *J. Gen. Physiol.* 104:507–522.

O'Leary, M.E., R.G. Kallen, and R. Horn. 1994. Evidence for a direct interaction between internal tetra-alkylammonium cations and the inactivation gate of cardiac sodium channels. *J. Gen. Physiol.* 104:523–539.

Pongs, O., N. Kecskemethy, R. Müller, I. Krah-Jentgens, A. Bauman, H.H. Kiltz, I. Canal, S. Llamazares, and A. Ferrus. 1988. *Shaker* encodes a family of putative potassium channel proteins in the nervous system of *Drosophila*. *EMBO (Eur. Mol. Biol. Organ.) J.* 7:1087–1096.

Qu, Y., J. Rogers, T. Tanada, T. Scheuer, and W.A. Catterall. 1995. Molecular determinants of drug access to the receptor site for antiarrhythmic drugs in the cardiac Na^+ channel. *Proc. Nat. Acad. Sci. USA.* 92:11839–11843.

Sine, S.M., and J.H. Steinbach. 1984. Agonists block currents through acetylcholine receptor channels. *Biophys. J.* 46:277–284.

Strichartz, G.R. 1973. The inhibition of sodium currents in myelinated nerve by quaternary derivatives of lidocaine. *J. Gen. Physiol.* 62:37–57.

Sun, Y.-M., I. Favre, L. Schild, and E. Moczydlowski. 1997. On the structural basis for size-selective permeation of organic cations through the voltage-gated sodium channel. Effect of alanine mutations at the DEKA locus on selectivity, inhibition by Ca^{2+}, and H^+, and molecular sieving. *J. Gen. Physiol.* 110:693–715.

Sunami, A., S.C. Dudley, Jr., and H.A. Fozzard. 1997. Sodium channel selectivity filter regulates antiarrhythmic drug binding. *Proc. Natl. Acad. Sci. USA.* 94:14126–14131.

Tasaki, I., and S. Hagiwara. 1957. Demonstration of two stable states in the squid giant axon under tetraethylammonium chloride. *J. Gen. Physiol.* 40:859–885.

Terlau, H., S.H. Heinemann, W. Stühmer, M. Pusch, F. Conti, K. Imoto, and S. Numa. 1991. Mapping the site of block by tetrodotoxin and saxitoxin of sodium channel II. *FEBS Lett.* 293:93–96.

Trimmer, J.S., S.S. Cooperman, S.A. Tomiko, J. Zhou, S.M. Crean, M.B. Boyle, R.G. Kallen, Z. Sheng, R.L. Barchi, F.J. Sigworth, et al. 1989. Primary structure and functional expression of a mammalian skeletal muscle sodium channel. *Neuron.* 3:33–49.

Wang, G.K. 1988. Cocaine-induced closures of single batrachotoxin-activated Na^+ channels in planar lipid bilayers. *J. Gen. Physiol.* 92:747–765.

Wang, G.K., R. Simon, and S.-Y. Wang. 1991. Quaternary ammonium compounds as structural probes of single batrachotoxin-activated Na^+ channels. *J. Gen. Physiol.* 98:1005–1024.

Williams, K. 1997. Interactions of polyamines with ion channels. *Biochem. J.* 325:289–297.

Woodhull, A.M. 1973. Ionic blockage of sodium channels in nerve. *J. Gen. Physiol.* 61:678–708.

Yamamoto, D., and J.Z. Yeh. 1984. Kinetics of 9-aminoacridine block of single Na channels. *J. Gen. Physiol.* 84:361–377.

Yang, J., P.T. Ellinor, W.A. Sather, J.-F. Zhang, and R.W. Tsien. 1993. Molecular determinants of Ca^{2+} selectivity and ion permeation in L-type Ca^{2+} channels. *Nature.* 366:158–161.

Yellen, G., M.E. Jurman, T. Abramson, and R. MacKinnon. 1991. Mutations affecting internal TEA blockade identify the probable pore-forming region of a K^+ channel. *Science.* 251:939–942.

Zamponi, G.W., D.D. Doyle, and R.J. French. 1993. Fast lidocaine block of cardiac and skeletal muscle sodium channels: one site with two routes of access. *Biophys. J.* 65:80–90.